Polish Academy of Sciences
Institute of Fundamental Technological Research

Archives of Mechanics

Archiwum Mechaniki Stosowanej

volume 55 issue 4

DRUKARNIA BRACI GRODZICKICH

SUBSCRIPTIONS

Address of the Editorial Office: Archives of Mechanics
Institute of Fundamental Technological Research, Świętokrzyska 21
PL 00-049 Warsaw, Poland
Tel. 48 (*prefix*) 22 826 60 22, Fax 48 (*prefix*) 22 826 98 15,
e-mail:publikac@ippt.gov.pl

Subscription orders for all journals edited by IFTR may be sent directly to the Editorial Office of the Institute of Fundamental Technological Research

Subscription rates

Annual subscription rate (2003) including postage is US $ 240.
Please transfer the subscription fee to our bank account: Payee: IPPT PAN,
Bank: PKO SA. IV O/Warszawa,
Account number 12401053-40054492-3000-401112-001.

All journals edited by IFTR are available also through:

- Foreign Trade Enterprise ARS POLONA Krakowskie Przedmieście 7,
  00-068 Warszawa, Poland fax 48 (*prefix*) 22 826 86 73

- RUCH S.A. ul. Towarowa 28,
  00-958 Warszawa, Poland fax 48 (*prefix*) 22 620 17 62

- International Publishing Service Sp. z o.o. ul. Noakowskiego 10 lok. 38
  00-664 Warszawa, Poland tel./fax 48 (*prefix*) 22 625 16 53, 625 49 55

Warunki prenumeraty

Redakcja przyjmuje prenumeratę na wszystkie czasopisma wydawane przez IPPT PAN. Bieżące numery można nabyć, a także zaprenumerować roczne wydanie Archiwum Mechaniki Stosowanej bezpośrednio w Dziale Wydawnictw IPPT PAN, Świętokrzyska 21, 00-049 Warszawa, Tel. 48 (*prefix*) 22 826 60 22; Fax 48 (*prefix*) 22 826 98 15.
Cena rocznej prenumeraty z bonifikatą (na rok 2003) dla krajowego odbiorcy wynosi 300 PLN

Również można je nabyć, a także zamówić (przesyłka za zaliczeniem pocztowym) we Wzorcowni Ośrodka Rozpowszechniania Wydawnictw Naukowych PAN,
00-818 Warszawa, ul. Twarda 51/55, tel. 48 (*prefix*) 22 697 88 35.
Wpłaty na prenumeratę przyjmują także jednostki kolportażowe RUCH S.A. Oddział Krajowej Dystrybucji Prasy, 00-958 Warszawa, ul. Towarowa 28. Konto: PBK. S.A. XIII Oddział Warszawa nr 11101053-16551-2700-1-67. Dostawa odbywa się pocztą lotniczą, której koszt w pełni pokrywa zleceniodawca. Tel. 48 (*prefix*) 22 620 10 39, Fax 48 (*prefix*) 22 620 17 62

Arkuszy wydawniczych 7,0. Arkuszy drukarskich 5,3.
Papier offset. kl III 70g. B1.
Druk ukończono w sierpniu 2003 r.
Skład w systemie TEX: E. Jaczyńska.
Druk i oprawa: Drukarnia Braci Grodzickich, Piaseczno ul. Geodetów 47A.

Arch. Mech., **55**, 4, pp. 327–344, Warszawa 2003

Non-Newtonian flows over an oscillating plate with variable suction

T. HAYAT, Q. ABBAS, M. KHAN, A. M. SIDDIQUI[1]

Department of Mathematics, Quaid-i-Azam University, Islamabad 45320, Pakistan

[1] *Department of Mathematics, Pennsylvania State University, York Campus, 1031 Edgecomb Avenue, York, PA 17403, U.S.A.*

THE FLOW OF second order fluid due to an oscillating infinite plate in the presence of a transverse magnetic field for two forms of time-dependent suction are considered. The analytical solutions of the governing boundary value problems are obtained. It is found that an external magnetic field and normal stress coefficient on the flow has opposite effects.

1. Introduction

IN THE PAST few years there has been a considerable interest in the oscillating flows due to possible applications in engineering. The study of such flows was first initiated by LIGHTHILL [1] who studied the effects of free-stream oscillations on the boundary layer flow of a viscous, incompressible fluid past an infinite plate. Thereafter STUART [2] extended it to study a two-dimensional flow past an infinite, porous plate with constant suction when the free-stream oscillates in time about a constant mean. The boundary layer suction is a very efficient method for the prevention of separation. The effects of different arrangements and configurations of the suction holes and slots on the undesired phenomenon of separation have been studied extensively by various scholars and have been compiled by LACHMANN [3].

Due to the development of practical boundary layer control systems, interest in problems concerning suction have been renewed. This problem has also been useful in the study of unsteady flow. Watson [4] generalized the Stuart's problem to the case of an arbitrary free-stream velocity. Later, KALONI [5] and MESSIHA [6] extended Stuart's problem to the case of constant and variable suction respectively. Further, SOUNDALGEKAR and PURI [7] discussed the fluctuating flow of an elastico-viscous fluid past an infinite plate with variable suction.

Using the viscous fluid model, the flow of a fluid near a porous oscillating infinite plane has been investigated in SCHLICHTING [8]. RAJAGOPAL [9, 10]

discussed the flows of second and third order fluids due to a rigid plate oscillating in its own plane. Later, FOOTE *et al.* [11] examined the flow of an oscillating porous plate for an elastico-viscous fluid. PURI [12] studied an oscillating rotating flow of an elastico-viscous fluid. Morerecently, HAYAT *et al.* [13–15] analyzed some periodic flows of a second order fluid. TURBATU *et al.* [16] generalized the viscous fluid flow problem of an oscillating flat plate in two directions. They first considered the oscillating flat plate with superimposed blowing or suction. The second generalization is concerned with an increasing or decreasing velocity amplitude of the oscillating flat plate.

On the other hand in view of the increasing technical applications using the magnetohydrodynamic effect, it is desirable to extend many of the available hydrodynamic solutions to include the effects of magnetic fields for those cases when the fluid is electrically conducting. Flow past a flat plate has been studied by ROSSOW [17]. He has considered transverse magnetic field on the flow. SURYAPRAKASRAO [18, 19] investigated the effects of transverse magnetic field on the fluctuating free-stream velocity when the plate is subjected to a constant suction velocity. Boundary layer flows of fluids of small electrical conductivity are important particularly in the field of aeronautical engineering. Further, in technological fields boundary layer phenomenon in non-Newtonian fluids is also being studied extensively. Therefore, it is of interest to analyze the effects of magnetic field on the flow of second order, incompressible and electrically conducting fluid over an infinite oscillating plate with variable suction.

The object of Sec. 2 is to investigate the effect of the variable suction velocity of the form $v_o'(1+ \in Ae^{i\omega' t'})$ as assumed by MESSIHA [6]. It is of interest to study how second order results get modified due to the conducting fluid over an oscillating porous plate. In Sec. 3 we assumed the suction velocity of the form $v_o[1+\delta(e^{i\omega t}+e^{-i\omega t})]$ as in KELLY [20]. Detailed study is made in order to extend the Kelly's results [20] of viscous fluid past an infinite plate with time dependent suction to the second order and electrically conducting fluid over an oscillating porous plate. Thus, in this section the combined effects of second order fluid and a magnetic field are considered.

2. Problem formulation

Consider the two dimensional flow of an incompressible and electrically conducting second order fluid over a porous oscillating plate of infinite extent, which occupies the plane $y' = 0$. The geometry of the problem is shown in the Fig. 1. Let u' and v' be the velocity components parallel and normal to the plate respectively. We look for a solution for the velocities which is independent of x', the distance parallel to the plate. Then the continuity equation requires that v' is at most a function of time and therefore retains its value at the plate throughout

the flow. Hence, following MESSIHA [6] and SOUNDALGEKAR [7] we consider v' for the first boundary value problem as

$$v' = -v'_{\circ}(1+ \in Ae^{i\omega' t'}), \tag{2.1}$$

where $v'_{\circ}$ is a non-zero constant mean suction velocity, ω' is the angular frequency, $\in$ is small and A is real positive constant such as $\in A \ll 1$. By neglecting higher powers of $\in$ approximate solutions are obtained for the velocity field in the boundary layer. The negative sign in Eq. (2.1) shows that the suction velocity normal to the wall is directed towards the wall. Further, the conducting fluid is permeated by an imposed uniform magnetic field $\mathbf{B} = [0, B_{\circ}, 0]$ which acts in the positive y'-direction normal to the sheet. In the low magnetic Reynolds number approximation (SHERCLIFF [22]), in which the induced magnetic field can be ignored, the magnetic body force $\mathbf{j} \times \mathbf{B}$ becomes $\sigma(\mathbf{V} \times \mathbf{B}) \times \mathbf{B}$ when imposed and induced electric fields are negligible and only the magnetic field $\mathbf{B}$ contributes to the current $\mathbf{j} = \sigma(\mathbf{V} \times \mathbf{B})$. Here, σ is the electrical conductivity of the fluid, which has density ρ'. The constitutive equation of a homogeneous incompressible fluid of second order is

$$\mathbf{T} = -p\mathbf{I} + \mu\mathbf{A}_1 + \alpha_1\mathbf{A}_2 + \alpha_2\mathbf{A}_1^2,$$

where $\mathbf{T}$ is the Cauchy stress tensor, $\mathbf{A}_1$ and $\mathbf{A}_2$ are the well known first two Rivlin-Ericken tensors, μ is the dynamic viscosity, α_1 and α_2 are normal stress moduli and p is the pressure. In view of $\mathbf{T}$ the momentum equation in absence of modified pressure gradient gives

$$\frac{\partial u'}{\partial t'} + v'\frac{\partial u'}{\partial y'} = \nu\frac{\partial^2 u'}{\partial y'^2} + \alpha^*\left[\frac{\partial^3 u'}{\partial y'^2 \partial t'} + v'\frac{\partial^3 u'}{\partial y'^3}\right] - \frac{\sigma B_{\circ}^2 u'}{\rho'}, \tag{2.2}$$

where

$$\nu = \frac{\mu}{\rho'}, \qquad \alpha^* = \frac{\alpha_1}{\rho'}.$$

In above equation α_1 is the material constant. For fluids to have motions which are compatible with thermodynamics in the sense of Clausius-Duhem inequality and the condition that the Helmholtz free energy be a minimum when the fluid is at rest, the following conditions must be satisfied [23]

$$\mu \geq 0, \qquad \alpha_1 \geq 0, \qquad \alpha_1 + \alpha_2 = 0.$$

The relevant boundary conditions for the problem are

$$u'(0, t') = U'_{\circ} \in e^{i\omega' t'}, \tag{2.3}$$

$$\lim_{y' \to \infty} u'(y', t') = 0. \tag{2.4}$$

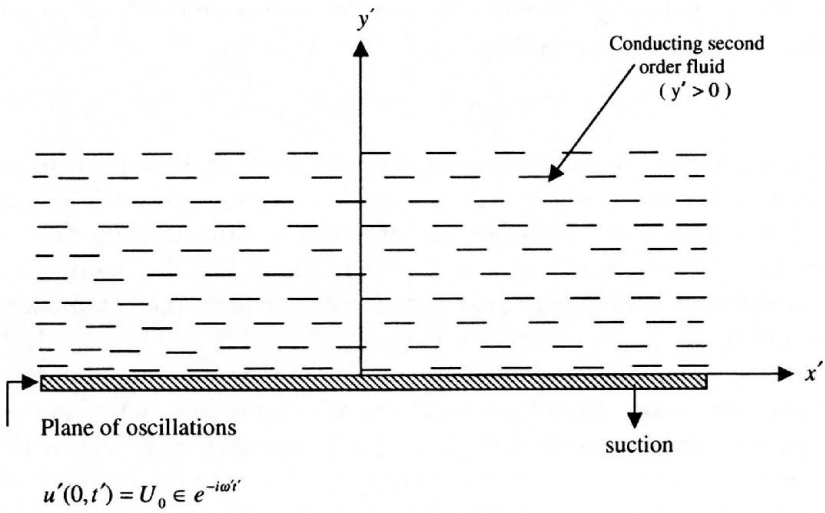

FIG. 1. Physical model under consideration.

It should be noted that for $\alpha_1 = B_\circ = 0$ we are left with the equations governing the flow of a non-conducting Newtonian fluid over an oscillating porous plate.

2.1. Solution of the first boundary value problem

Following [7] we take a solution of the form

$$u'(y',\, t') = U'_\circ \left[f_1(y') + \in e^{i\omega' t'} f_2(y') \right]. \tag{2.5}$$

Now using Eqs. (2.1) and (2.5) in Eqs. (2.2) to (2.4), comparing harmonic and non-harmonic terms and neglecting coefficients of $\in^2$, we get

$$\alpha \frac{d^3 f_1}{d\eta^3} - \frac{d^2 f_1}{d\eta^2} - \frac{df_1}{d\eta} + N f_1 = 0, \tag{2.6}$$

$$\alpha \frac{d^3 f_2}{d\eta^3} - \left(1 + \frac{1}{4} i\omega\alpha\right) \frac{d^2 f_2}{d\eta^2} - \frac{df_2}{d\eta} + \left(\frac{i\omega}{4} + N\right) f_2 = A \frac{df_1}{d\eta} - \alpha A \frac{d^3 f_1}{d\eta^3}, \tag{2.7}$$

$$\begin{aligned} &f_1 = 0, \quad f_2 = 1, \quad \text{at } \eta = 0, \\ &f_1 = 0, \quad f_2 = 0, \quad \text{as } \eta \to \infty, \end{aligned} \tag{2.8}$$

where

$$\eta = \frac{y'v'_\circ}{\nu}, \qquad t = \frac{v'^2_\circ t'}{4\nu}, \qquad \omega = \frac{4\nu\omega'}{v'^2_\circ},$$
$$u = \frac{u'}{U'_\circ}, \qquad \alpha = \frac{\alpha^* v'^2_\circ}{\nu^2}, \qquad N = \frac{\sigma\nu B^2_\circ}{\rho' v'^2_\circ}. \tag{2.9}$$

During the past three decades there have been several studies of boundary layer flows of non-Newtonian fluids. These investigations have been for non-Newtonian fluids of the differential type [24]. In the case of fluids of differential type, the equations of motion are an order higher than the Navier-Stokes equations and thus the adherence boundary condition is insufficient to determine the solution completely (see [25–27] for a detailed discussion of the relevant issues). The same is also true for the approximate boundary layer approximations of motion. In the absence of a clear means of obtaining additional boundary conditions, BEARD and WALTERS [28], in their study of an incompressible fluid of elastico-viscous suggested a method for overcoming this difficulty. They suggested a perturbation approach in which the velocity and the pressure field were expanded in a series in terms of small parameter. This parameter in question multiplied the highest order spatial derivatives in their equation. Though this approximation reduces the order of the equation, it treats a singular perturbation problem as a regular perturbation problem.

In 1991, GARG and RAJAGOPAL suggested that it would be preferable to overcome the difficulty associated with the paucity of boundary conditions by augmenting them on the basis of physically reasonable assumptions. They thought that it is possible to do this in the case of flows which take place in unbounded domains by using the fact that either the solution is bounded or the solution has certain smoothness at infinity. To demonstrate this, GARG and RAJAGOPAL [29] studied the stagnation flow of a fluid of second order by augmenting the boundary conditions. Their result agreed well with the result of RAJESWARI and RATHNA [30] who studied the problem based on the perturbation approach for a small value of the perturbation parameter.

Before proceeding with the solution, we note that Eqs. (2.6) and (2.7) are the third-order differential equations when $\alpha \neq 0$ and for the classical viscous case ($\alpha = 0$), we encounter differential equations of order two. Hence the presence of the material constant of the fluid increases the order of the governing equations from two to three. It would, therefore, seem that an additional boundary condition must be imposed in order to get a unique solution. The difficulty, in the present case, in however, removed by seeking a solution of the form [28]

$$f_1 = f_{01} + \alpha f_{11} + O(\alpha^2),$$
$$f_2 = f_{02} + \alpha f_{12} + O(\alpha^2), \tag{2.10}$$

which is valid for small values of α. Putting Eqs. (2.10) in Eqs. (2.6), (2.7) and boundary conditions (2.8) and equating the coefficients of α and then solving the resulting boundary value problems, the velocity field is given by

$$u = (1 + \alpha L\eta) \in e^{-h\eta + i\omega t}, \tag{2.11}$$

where

$$h = h_r + ih_i = \frac{1 + \sqrt{1 + 4N + i\omega}}{2},$$

$$L = L_r + iL_i = \frac{h^2\left(h + \frac{i\omega}{4}\right)}{\sqrt{1 + 4N + i\omega}}. \tag{2.12}$$

Knowing the velocity field, we now calculate the shearing stress which in terms of η is given by

$$p_{xy} = \frac{p'_{x'y'}}{U'_o v'_o \rho'} = \frac{\partial u}{\partial \eta} + \frac{\alpha}{4}\left[\frac{\partial^2 u}{\partial \eta \partial t} - 4\left(1 + \in Ae^{i\omega t}\right)\frac{\partial^2 u}{\partial \eta^2}\right]. \tag{2.13}$$

From Eqs. (2.11) and (2.13) we get

$$(p_{xy})_{\eta \to 0} = \in e^{i\omega t}\left[\alpha L - h - \frac{i\omega}{4}\alpha h - \alpha h^2\right]. \tag{2.14}$$

Now from Eqs. (2.11) and (2.14) we have

$$u(y, t) = (M_r \cos \omega t - M_i \sin \omega t), \tag{2.15}$$

$$p_{xy} = |B| \cos(\omega t + \beta), \tag{2.16}$$

where

$$M_r = \in e^{-h_r \eta}\left[\cos h_i\eta + \alpha\eta\left(L_r \cos h_i\eta + L_i \sin h_i\eta\right)\right], \tag{2.17}$$

$$M_i = -\in e^{-h_r \eta}\left[\sin h_i\eta - \alpha\eta\left(L_i \cos h_i\eta - L_r \sin h_i\eta\right)\right], \tag{2.18}$$

$$B = B_r + iB_i, \qquad \beta = \arctan\frac{B_i}{B_r},$$

$$B_r = \in\left[\alpha L_r - h_r + \frac{1}{4}\omega\alpha h_i - \alpha\left(h_r^2 - h_i^2\right)\right],$$

$$B_i = \in\left[\alpha L_i - h_i - \frac{1}{4}\omega\alpha h_r - 2\alpha h_r h_i\right], \tag{2.19}$$

$$h_i = \frac{1}{2}\left[\frac{1}{2}\left\{\sqrt{(1+4N)^2+\omega^2}-1-4N\right\}\right]^{1/2},$$

$$h_r = \frac{1}{2}+\frac{1}{2}\left[\frac{1}{2}\left\{\sqrt{(1+4N)^2+\omega^2}+1+4N\right\}\right]^{1/2}, \tag{2.20}$$

$$L_r = \frac{1}{2}+\frac{N}{2}+\frac{a}{2}+\frac{N\omega b}{4r}-\frac{Na}{2r}-\frac{\omega^2 a}{16r},$$

$$L_i = \frac{\omega}{4}+\frac{b}{2}+\frac{N\omega a}{4r}+\frac{Nb}{2r}+\frac{\omega^2 b}{16r}, \tag{2.21}$$

$$r = a^2+b^2 = \sqrt{(1+4N)^2+\omega^2}, \tag{2.22}$$

$$a = \sqrt{\frac{\sqrt{(1+4N)^2+\omega^2}+1+4N}{2}},$$

$$b = \sqrt{\frac{\sqrt{(1+4N)^2+\omega^2}-1-4N}{2}}. \tag{2.23}$$

3. Second boundary value problem

In this section geometry of the problem is the same as that in the previous section except the form of the variable suction velocity. Thus, following the notation of [20], the boundary layer equation with no pressure gradient is given by

$$\frac{\partial u}{\partial t}+v_o\left[1+\delta\left(e^{i\omega t}+e^{-i\omega t}\right)\right]\frac{\partial u}{\partial y} = \nu\frac{\partial^2 u}{\partial y^2}+\alpha^*\left[\frac{\partial^3 u}{\partial y^2\partial t}+v_o\left\{1+\delta\left(e^{i\omega t}+e^{-i\omega t}\right)\right\}\frac{\partial^3 u}{\partial y^3}\right]-\frac{\sigma B_o^2 u}{\rho}, \tag{3.1}$$

where $\nu = \mu/\rho$, $\alpha^* = \alpha_1/\rho$, $v_o < 0$ is the suction at the wall and the coupling parameter is the non-dimensional amplitude, say, δ. Note that in writing Eq. (3.1) we have used the variable suction velocity equal to $v_o[1+\delta(e^{i\omega t}+e^{-i\omega t})]$ from KELLY [20]. We further note that for $\alpha^* = 0 = B_o$ Eq. (3.1) reduces to KELLY [20]. For the problem under consideration the boundary conditions are

$$u(0,\ t) = 2U_o\cos\omega t, \tag{3.2}$$

$$u(\infty,\ t) = 0. \tag{3.3}$$

3.1. Solution of the second boundary value problem

We shall assume a solution of the form

$$u(y,\ t) = u_0(y) + \sum_{n=1}^{\infty} u_n(y)\, e^{in\omega t} + \sum_{n=1}^{\infty} \tilde{u}_n(y)\, e^{-in\omega t}, \tag{3.4}$$

where $\tilde{u}_n(y)$ is the complex conjugate of $u_n(y)$. Substituting Eq. (3.4) in (3.1) to (3.3) and then introducing

$$\eta = \frac{|v_\circ|\, y}{\nu}, \qquad u_n = U_\circ \phi_n, \tag{3.5}$$

into the resulting equations and the boundary conditions we arrive at the following boundary value problems

$$\frac{v_\circ}{|v_\circ|}\frac{d\phi_0}{d\eta} + \frac{\delta v_\circ}{|v_\circ|}\left(\frac{d\phi_1}{d\eta} + \frac{d\,\tilde{\phi}_1}{d\eta}\right) = \frac{d^2\phi_0}{d\eta^2} + \alpha\frac{v_\circ}{|v_\circ|}\frac{d^3\phi_0}{d\eta^3} + \alpha\frac{\delta v_\circ}{|v_\circ|}\left(\frac{d^3\phi_1}{d\eta^3} + \frac{d^3\,\tilde{\phi}_1}{d\eta^3}\right) - N_1\phi_0, \tag{3.6}$$

$$\phi_0(0) = 0, \qquad \phi_0(\infty) = 0, \tag{3.7}$$

$$in\lambda\phi_n + \frac{v_\circ}{|v_\circ|}\frac{d\phi_n}{d\eta} + \frac{\delta v_\circ}{|v_\circ|}\left(\frac{d\phi_{n-1}}{d\eta} + \frac{d\phi_{n+1}}{d\eta}\right) = \frac{d^2\phi_n}{d\eta^2} + \alpha\frac{\delta v_\circ}{|v_\circ|}\left(\frac{d^3\phi_{n-1}}{d\eta^3} + \frac{d^3\phi_{n+1}}{d\eta^3}\right) + \alpha\frac{v_\circ}{|v_\circ|}\frac{d^3\phi_n}{d\eta^3} + in\alpha\lambda\frac{d^2\phi_n}{d\eta^2} - N_1\phi_0, \quad n \geq 1, \tag{3.8}$$

$$\phi_1(0) = 1, \qquad \phi_1(\infty) = 0, \tag{3.9}$$

$$\phi_n(0) = 0, \qquad \phi_n(\infty) = 0, \qquad n \geq 2, \tag{3.10}$$

where

$$\alpha = \frac{\alpha^*\,|v_\circ|^2}{\nu^2}, \qquad \lambda = \frac{\omega\nu}{|v_\circ|^2}, \qquad N_1 = \frac{\nu\sigma B_\circ^2}{\rho\,|v_\circ|^2}. \tag{3.11}$$

Equations similar to (3.8) to (3.10) result for $\tilde{\phi}_1$ and $\tilde{\phi}_n$.

For $\delta \ll 1$, the equations are weakly coupled and an expansion is performed in terms of powers of δ. Hence, we define

$$\phi_n(\eta) = \sum_{j=0}^{\infty} \phi_{nj}(\eta)\, \delta^j. \tag{3.12}$$

Making use of (3.11) in (3.6) to (3.10) and then comparing the powers of δ we get

$$\alpha \frac{d^3\phi_{00}}{d\eta^3} - \frac{d^2\phi_{00}}{d\eta^2} + \frac{v_\circ}{|v_\circ|}\frac{d\phi_{00}}{d\eta} + N_1\phi_{00} = 0, \tag{3.13}$$

$$\phi_{00}(0) = 0, \qquad \phi_{00}(\infty) = 0,$$

$$\alpha \frac{d^3\phi_{10}}{d\eta^3} - (1 + i\alpha\lambda)\frac{d^2\phi_{10}}{d\eta^2} - \frac{d\phi_{10}}{d\eta} + (i\lambda + N_1)\phi_{10} = 0, \tag{3.14}$$

$$\phi_{10}(0) = 1, \qquad \phi_{10}(\infty) = 0,$$

$$\alpha \frac{d^3\phi_{01}}{d\eta^3} - \frac{d^2\phi_{01}}{d\eta^2} - \frac{d\phi_{01}}{d\eta} + N_1\phi_{01} = \left(\frac{d\phi_{10}}{d\eta} + \frac{d\,\widetilde{\phi}_{10}}{d\eta}\right) - \alpha\left(\frac{d^3\phi_{10}}{d\eta^3} + \frac{d^3\,\widetilde{\phi}_{10}}{d\eta^3}\right), \tag{3.15}$$

$$\phi_{01}(0) = 0, \qquad \phi_{01}(\infty) = 0,$$

$$\alpha \frac{d^3\phi_{11}}{d\eta^3} - (1 + i\alpha\lambda)\frac{d^2\phi_{11}}{d\eta^2} - \frac{d\phi_{11}}{d\eta} + (i\lambda + N_1)\phi_{11} = -\alpha\left(\frac{d^3\phi_{00}}{d\eta^3} + \frac{d^3\phi_{20}}{d\eta^3}\right) + \left(\frac{d\phi_{00}}{d\eta} + \frac{d\phi_{20}}{d\eta}\right), \tag{3.16}$$

$$\phi_{11}(0) = 0, \qquad \phi_{11}(\infty) = 0,$$

$$\alpha \frac{d^3\phi_{02}}{d\eta^3} - \frac{d^2\phi_{02}}{d\eta^2} - \frac{d\phi_{02}}{d\eta} + N_1\phi_{02} = \left(\frac{d\phi_{11}}{d\eta} + \frac{d\,\widetilde{\phi}_{11}}{d\eta}\right) - \alpha\left(\frac{d^3\phi_{11}}{d\eta^3} + \frac{d^3\,\widetilde{\phi}_{11}}{d\eta^3}\right), \tag{3.17}$$

$$\phi_{02}(0) = 0, \qquad \phi_{02}(\infty) = 0.$$

Similar to (2.10) we can write

$$\begin{aligned}
\phi_{00} &= \phi_{00,1} + \alpha\phi_{00,2} + O\left(\alpha^2\right), \\
\phi_{10} &= \phi_{10,1} + \alpha\phi_{10,2} + O\left(\alpha^2\right), \\
\phi_{01} &= \phi_{01,1} + \alpha\phi_{01,2} + O\left(\alpha^2\right), \\
\phi_{11} &= \phi_{11,1} + \alpha\phi_{11,2} + O\left(\alpha^2\right), \\
\phi_{02} &= \phi_{02,1} + \alpha\phi_{02,2} + O\left(\alpha^2\right).
\end{aligned} \tag{3.18}$$

Substituting (3.18) in (3.13) to (3.16), equating the coefficients of α and then solving the resulting systems we arrive at

$$\phi_{n0} = 0, \qquad n = 0 \qquad \text{and} \qquad n \geq 2, \tag{3.19}$$

$$\phi_{10} = (1 + \alpha S\eta)\, e^{-g\eta}, \tag{3.20}$$

$$\phi_{11} = 0, \tag{3.21}$$

$$\phi_{02} = 0, \tag{3.22}$$

$$\phi_{01} = -\left(\frac{2}{\lambda} g_i + \alpha A_0 + \frac{2}{\lambda}\alpha\eta g_i\right) e^{-\eta} + Q_r \cos g_i\eta + Q_i \sin g_i\eta\,, \tag{3.23}$$

where

$$A_\circ = -\frac{2}{\lambda^2}\left[(2 + g_r)\,\lambda^2 + \lambda\,(3g_i - S_i) - g_r + (S_r g_r - S_i g_i)\right],$$

$$g = g_r + ig_i = \frac{1 + \sqrt{1 + 4N_1 + 4i\lambda}}{2},$$

$$S = S_r + iS_i = \frac{g^2\,(g + i\lambda)}{\sqrt{1 + 4N_1 + 4i\lambda}},$$

$$\begin{aligned}
Q_r = \frac{2}{\lambda^2} e^{-g_r\eta}\Big[&- \alpha\lambda^2\,(2 + g_r) + \lambda g_i - \alpha\lambda\{(3g_i - S_i) \\
&- \eta\,(S_r g_i + S_i g_r)\} + \alpha g_r - \alpha\,(S_r g_r - S_i g_i)\Big],
\end{aligned}$$

$$Q_i = \frac{2}{\lambda^2} e^{-g_r\eta}\Big[-\alpha\lambda^2 g_i - \lambda g_r + \alpha\lambda\{3g_r - S_r + 1 - \eta(S_r g_r - S_i g_i)\} - \alpha g_i + \alpha(S_r g_i + S_i g_r)\Big].$$

Hence from (3.4), (3.5), (3.12) and (3.19) to (3.23); the velocity field in the boundary layer is given by

$$u = U_\circ[\{(-\frac{2}{\lambda} g_i - \alpha A_\circ - \frac{2}{\lambda}\alpha\eta g_i)e^{-\eta} + Q_r \cos g_i\eta + Q_i \sin g_i\eta\}\delta + e^{-g_r\eta}\cos(g_i\eta - \omega t) + e^{-g_r\eta}\alpha\eta\{S_r\cos(g_i\eta - \omega t) + S_i \sin(g_i\eta - \omega t)\}]. \tag{3.24}$$

The expression for the shearing stress in term of η is given by

$$P_{xy} = \rho U_\circ |v_\circ| \left[\frac{\partial\phi}{\partial\eta} + \alpha\left[\frac{\lambda}{\omega}\frac{\partial^2\phi}{\partial\eta\partial t} - v_\circ\{1 + \delta(e^{i\omega t} + e^{-i\omega t})\}\frac{\partial^2\phi}{\partial\eta^2}\right]\right]. \tag{3.25}$$

Using (3.5) and (3.24) in (3.25) and neglecting $O(\delta^2)$ terms we get

$$(P_{xy})_{\eta\to 0} = \rho U_\circ |v_\circ| [|E| \cos(\omega t + \gamma) - 2\delta], \tag{3.26}$$

where

$$E^2 = E_1^2 + E_2^2, \qquad \gamma = \arctan\frac{E_2}{E_1},$$

$$E_1 = -g_r + \alpha(S_r + \lambda g_i - g_r),$$

$$E_2 = g_i - \alpha(S_i + \lambda g_r + g_i + \lambda),$$

$$g_i = \frac{1}{2}\left[\frac{1}{2}\left\{\sqrt{(1+4N_1)^2 + 16\lambda^2} - 1 - 4N_1\right\}\right]^{\frac{1}{2}},$$

$$g_r = \frac{1}{2} + \frac{1}{2}\left[\frac{1}{2}\left\{\sqrt{(1+4N_1)^2 + 16\lambda^2} + 1 + 4N_1\right\}\right]^{\frac{1}{2}}, \tag{3.27}$$

$$S_r = \frac{1}{2} + \frac{N_1}{2} + \frac{a_1}{2} + \frac{N_1\lambda b_1}{r_1} - \frac{N_1 a_1}{2r_1} - \frac{\lambda^2 a_1}{r_1},$$

$$S_i = \lambda + \frac{b_1}{2} + \frac{N_1\lambda a_1}{r_1} + \frac{N_1 b_1}{2r_1} + \frac{\lambda^2 b_1}{r_1},$$

$$r_1 = a_1^2 + b_1^2 = \sqrt{(1+4N_1)^2 + 16\lambda^2},$$

$$a_1 = \sqrt{\frac{\sqrt{(1+4N_1)^2 + 16\lambda^2} + 1 + 4N_1}{2}},$$

$$b_1 = \sqrt{\frac{\sqrt{(1+4N_1)^2 + 16\lambda^2} - 1 - 4N_1}{2}}.$$

4. Discussions

In order to investigate the effects of the material parameter on the flow we have plotted u against η in Figs. 2 to 7.

- In Fig. 2 we note that the boundary layer thickness decreases with increase in frequency. It is further noted form Fig. 3 that velocity is negative for higher values of ω when $N = 100$.
- Figure 4 indicates the variation of the velocity profile for various values of α. It is observed that as α increases, the value of the velocity decreases. That is, increasing the normal stress coefficient has the effect of increasing the boundary layer thickness. Further, comparison of Figs. 4 and 5 show that layer thickness decreases drastically with increase of N. It appears that the electromagnetic force makes the layer thicknesses thinner. It is likely that the magnetic field provides some mechanism to control the growth of the boundary layer thickness. Moreover, Fig. 5 also illustrates that u is negative for $\omega t = \pi/2$, $\in = 0.5$, $\omega = 10$, $N = 100$, $\alpha = 0.025,\ 0.05,\ 0.075,\ 0.1$.
- In Figs. 6 and 7, the effect of material parameter is shown for second problem when $N = 0$ and $N \neq 0$ respectively. It is also clear from Fig. 6 that u decreases with increase of α first and then increases. With $N \neq 0$ in Fig. 7, the velocity is less in comparison to the velocity in Fig. 6.
- In Figs. 8 and 9 the fluctuating parts are shown for comparison purposes when $N = 5, \in = 0.5$ and $\omega = 100$. Figure 9 is particularly interesting because it illustrates the effects of α at large ω on M_i. In the case of fluids with material parameter, at $\omega = 100$, there is a sudden rise and fall of M_i near the wall. Also, from Figs. 8 and 9 one can conclude that an increase in α leads to much increase in M_i than M_r.

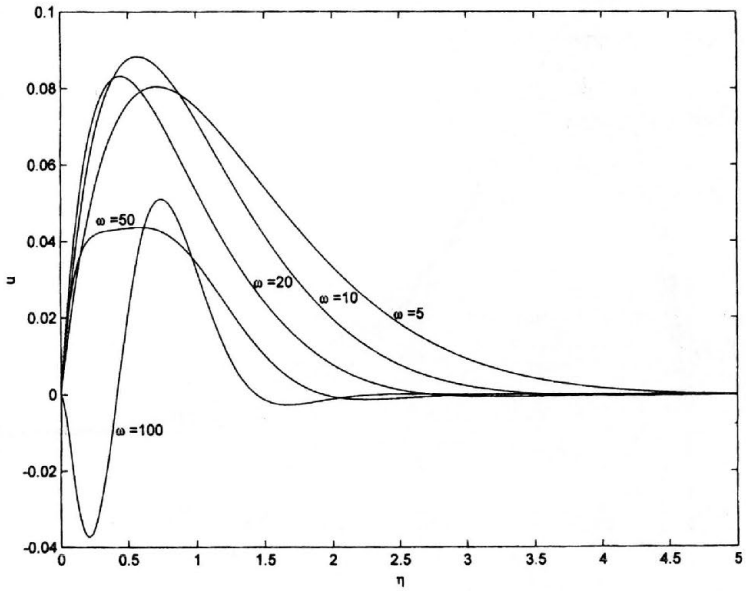

FIG. 2. Normalized velocity profiles for first BVP $\omega t = \pi/2$, $\varepsilon = 0.5$, $\alpha = 0.05$, $N = 0$.

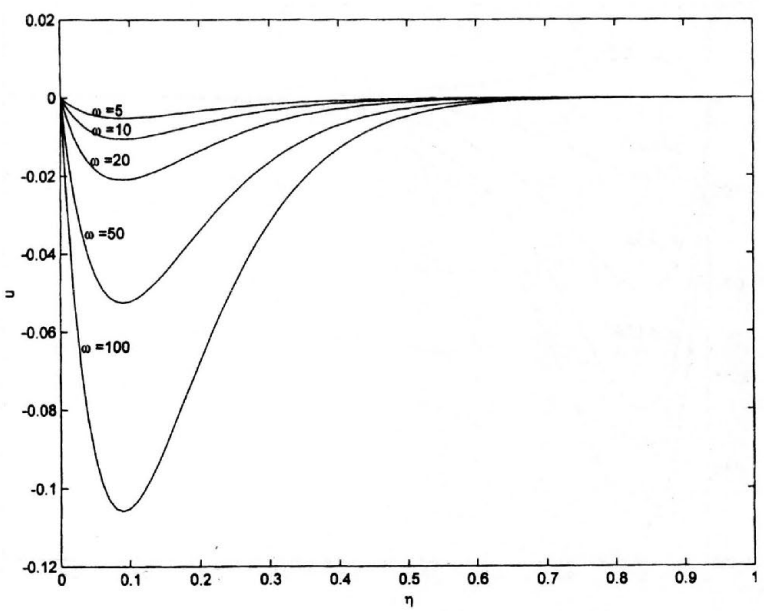

FIG. 3. Normalized velocity profiles for first BVP $\omega t = \pi/2$, $\varepsilon = 0.5$, $\alpha = 0.05$, $N = 100$.

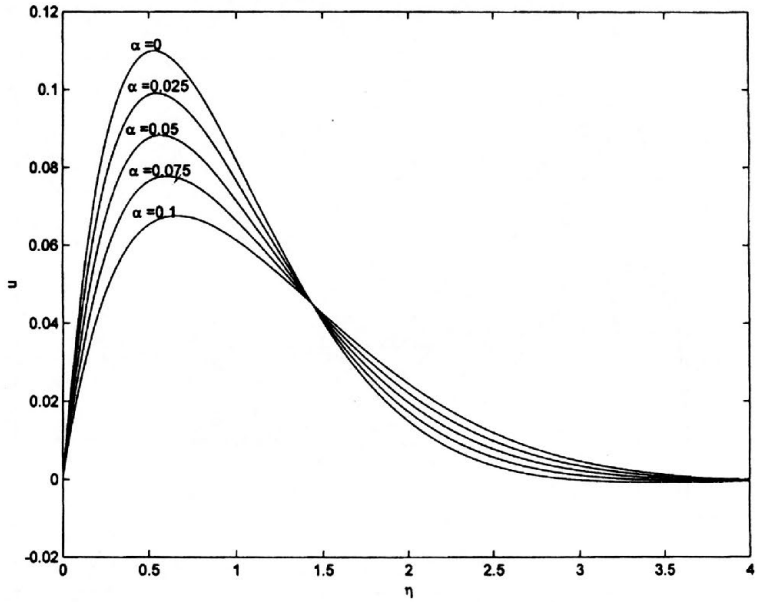

FIG. 4. Normalized velocity profiles for first BVP $\omega t = \pi/2,\ \varepsilon = 0.5,\ \omega = 10,\ N = 0.$

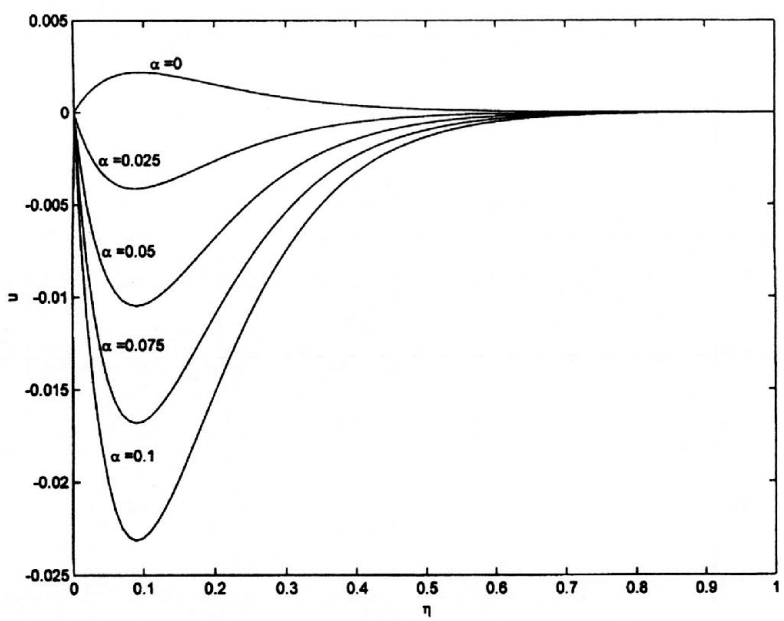

FIG. 5. Normalized velocity profiles for first BVP $\omega t = \pi/2,\ \varepsilon = 0.5,\ \omega = 10,\ N = 100.$

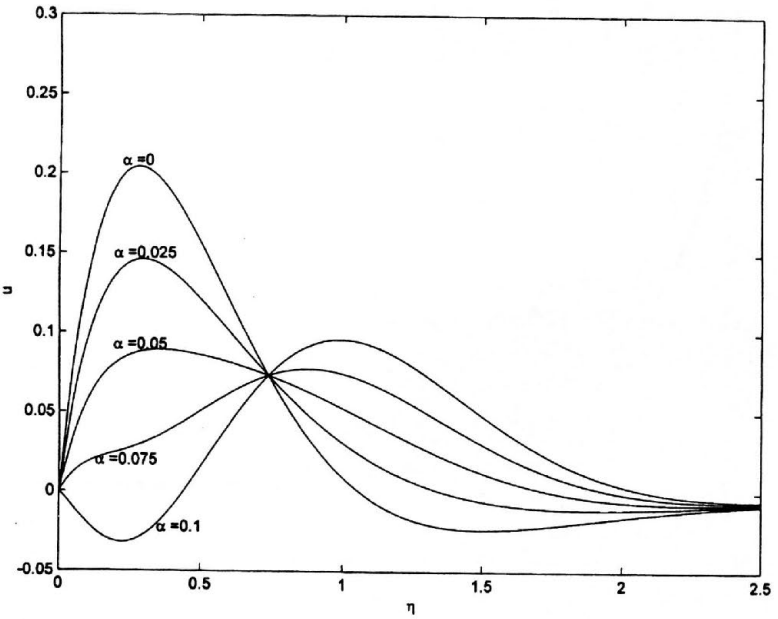

FIG. 6. Normalized velocity profiles for second BVP $\omega t = \pi/2,\ \delta = 0.2,\ \lambda = 10,\ N = 0.$

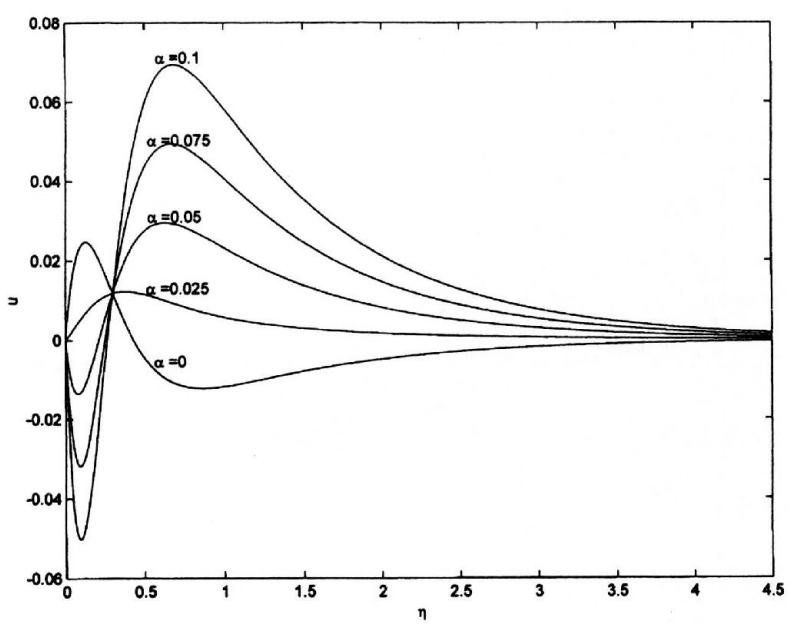

FIG. 7. Normalized velocity profiles for second BVP $\omega t = \pi/2,\ \delta = 0.2,\ \lambda = 10,\ N = 30.$

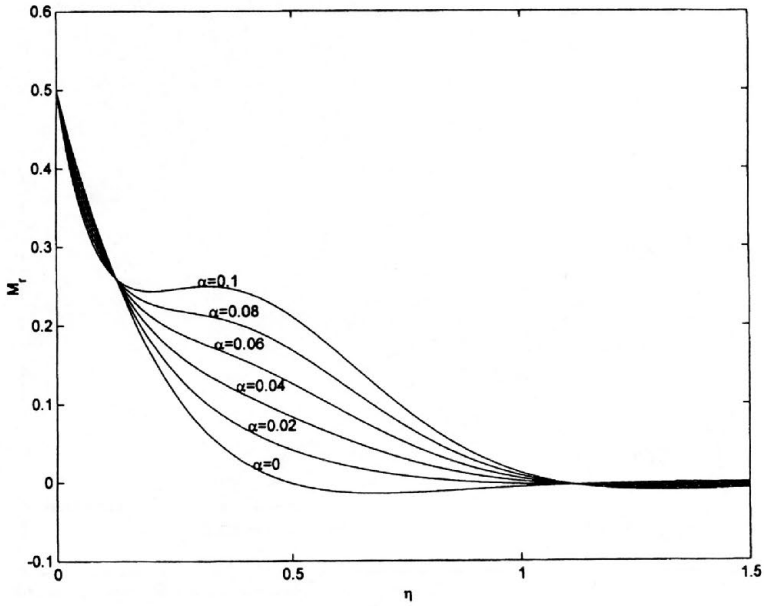

FIG. 8. Fluctuating part M_r at $\varepsilon = 0.5,\ \omega = 100,\ N = 5$.

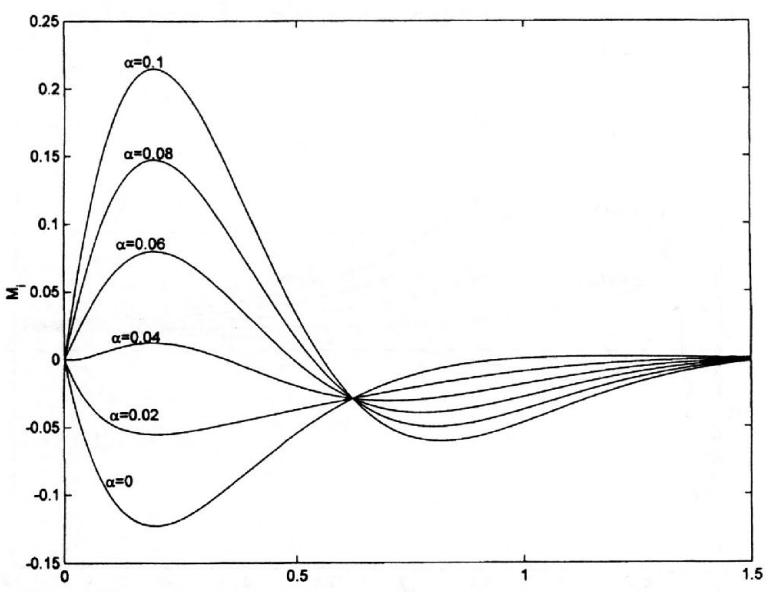

FIG. 9. Fluctuating part M_i at $\varepsilon = 0.5,\ \omega = 100,\ N = 5$.

5. Concluding remarks

Exact solutions for the Stokes problem on a porous plate for an second order fluid are obtained in the presence of a magnetic field. From Eqs. (2.15), (2.17), (2.18), (3.24) and (3.27), it is found that the penetration depth decreases with fundamental frequency. This is not surprising; if we slowly oscillate a plate in a sticky fluid, we expect to drag large masses of fluid along with the plate; on the other hand, if we move the plate rapidly in a fluid of low viscosity, we expect the fluid essentially to ignore the plate, except in a thin boundary layer. Further, we note from these solutions that an increase of the magnetic field reduces the velocity within the boundary layer and also to reduce the boundary layer thickness.

References

1. M. J. LIGHTHILL, *The response of laminar skin friction and heat transfer to fluctuations in the stream velocity*, Proc. R. Soc. Lond., **A224**, 1, 1954.
2. J. T. STUART, *A solution of the Navier-Stokes and energy equations illustrating the response of skin friction and temperature of an infinite plate thermometer to fluctuations in the stream velocity*, Proc. R. Soc. Lond., **A231**, 116, 1955.
3. G. V. LACHMANN, *Boundary layer and flow contro, its principles and applications*, vols. I and II, Pergamon Press, Oxford 1961.
4. J. WATSON, *A solution of the Navier-Stokes equation illustrating the response of the laminar boundary layer to a given change in the external stream velocity*, Quart. J. Mech. Appl. Math., **11**, 302, 1958.
5. P. N. KALONI, *Fluctuating flow of an elastico-viscous fluid past a porous flat plate*, Physics of Fluids., **10**, 1344, 1966.
6. S. A. S. MESSIHA, *Laminar boundary layers in oscillating flow along an infinite flat plate with variable suction*, Proc. Camb. Phil. Soc., **62**, 329, 1966.
7. V. M. SOUNDALGEKAR, P. PURI, *On fluctuating flow of an elastico-viscous fluid past an infinite plate with variable suction*, J. Fluid Mech., **35**, 3, 561, 1969.
8. H. SCHLICHTING, *Grenzschicht theorie*, 8-th edition, Braun, Karlsruhe 1982.
9. K. R. RAJAGOPAL, *A note on unsteady unidirectional flows of a non-Newtonian fluid*, Int. J. Non-Linear Mech., **17**, 369, 1982.
10. K. R. RAJAGOPAL, T. Y. NA, *On Stokes problem for a non-Newtonian fluid*, Acta Mech., **48**, 233, 1983.
11. J. R. FOOTE, P. PURI, P. K. KYTHE, *Some exact solutions of the Stokes problem for an elastico-viscous fluid*, Acta Mech., **68**, 233, 1987.
12. P. PURI, *Rotating flow of an elastico-viscous fluid on an oscillating plate*, ZAMM., **54**, 743, 1974.
13. T. HAYAT, S. ASGHAR, A. M. SIDDIQUI, *Periodic unsteady flows of a non-Newtonian fluid*, Acta Mech., **131**, 169, 1998.

14. T. HAYAT, S. ASGHAR, A. M. SIDDIQUI, *On the moment of a plane disk in a non-Newtonian fluid*, Acta Mech., **136**, 125, 1999.

15. T. HAYAT, S. ASGHAR, A. M. SIDDIQUI, *Some non steady flows of non-Newtonian fluid*, Int. J. Engng. Sci., **38**, 337, 2000.

16. S. TURBATU, K. BUHLER, J. ZIEREP, *New solutions of the II-Stokes problem for an oscillating flat plate*, Acta Mech., **129**, 25, 1998.

17. V. J. ROSSOW, NASA Tech. Note 3971, 1957.

18. U. SURYAPRAKASARAO, *The reponse of laminar skin friction and heat transfer to fluctuations in the stream velocity in the presence of a transverse magnetic field*, I. Z. Angew. Math. Mech., **43**, 133, 1962.

19. IBID, II Z. Angew. Math. Mech., **43**, 127, 1963.

20. R. E. KELLY *The flow of a viscous fluid past a wall of infinite extent with time-dependent suction*, Quart. J. Mech. Appl. Math., **18**, 13, 287, 1965.

21. K. WALTERS, in IUTAM. International Symposium on second order effects in elasticity, *Plasticity and fluid dynamic*, M. REINER and D. ABIR, [Eds.], Pergamon Press., Inc., 507, New York 1964.

22. J. A. SHERCLIFF, *A text book of magnetohydrodynamics*, Pergamon Press, 1965.

23. J. E. DUNN, R. L. FOSDICK, *Thermodynamics stability and boundedness of fluids of complexity 2 and fluids of second grade*, Arch. Rat. Mech. Anal., **3**, 191, 1974.

24. C. TRUESDELL, W. NOLL, *The nonlinear field theories of mechanics* (Handbuch der Physik, III/3), Berlin Heidelberg New York Springer, 1965.

25. K. R. RAJAGOPAL, *On boundary conditions for fluids of differential type*, [in:] A. SEQUEIRA [Ed.], *Navier-Stokes equations and related nonlinear problems*, Plenum Press, 273, New York 1995.

26. K. R. RAJAGOPAL, P. N. KALONI, *Some remarks on boundary conditions for differential type*, [in:] G. A. C. GRAHAM, S. K. MALIK, [Eds.], Continum mechanics and its applications, 936, Heimsphere, New York 1989.

27. K. R. RAJAGOPAL, A. S. GUPTA, *An exact solution for the flow of non-Newtonian fluid past an infinite plate*, Meccanica, **19**, 158, 1984.

28. W. D. BEARD, K. WALTERS, *Elastico-viscous boundary-layer flows*, Proc. Camb. Phil. Soc., **60**, 667, 1964.

29. V. K. GARG, K. R. RAJAGOPAL, *Flow of non-Newtonian fluid past a wedge*, Acta Mech., **88**, 113, 1991.

30. G. K. RAJESWARI, S. L. RATHNA, *Flow of a particular class of non-Newtonian visco-elastic and visco-elastic fluids near a stagnation point*, ZAMP., **13**, 43, 1962.

Received August 26, 2002; revised version April 10, 2003.

Arch. Mech., **55**, 4, pp. 345–355, Warszawa 2003

Variable viscosity and thermal conductivity effects on heat transfer by natural convection from a cone and a wedge in porous media

I. A. HASSANIEN[1], A. H. ESSAWY[2], N. M. MOURSY[2]

[1] *Assuit University, Faculty of Science, Department of Mathematics, Assuit, Egypt*

[2] *Minia University, Faculty of Science, Department of Mathematics, Minia, Egypt*

THE PROBLEM OF STEADY, laminar heat transfer by natural convection flow over a vertical cone and a wedge embedded in a uniform porous medium with variable viscosity and thermal conductivity is investigated. The transformed governing equations are solved numerically by using a finite difference scheme. The obtained results are compared with earlier papers on special cases of the problem and are found to be in excellent agreement. The influence of porous medium inertia effect, viscosity variation parameter ϵ and thermal conductivity variation parameter γ on the fluid velocity and temperature is discussed. Including the porous medium inertia effect or viscosity variation parameter in the mathematical model is predicted to reduce the local Nusselt number. Furthermore, the local Nusselt number increases in the presence of thermal conductivity variation parameter.

Notations

c_p specific heat,
f dimensionless stream function,
F inertia coefficient of the porous medium,
g gravitational acceleration,
h local heat transfer coefficient,
K permeamility of the porous media,
κ thermal conductivity of the porous medium,
κ_f thermal conductivity of the ambient fluid,
n geometric factor,
Nu_x local Nusselt number,
Ra_x local Raleigh number, $\dfrac{g\cos\gamma_1\beta_T K(T_w - T_\infty)x}{\mu_f \alpha_e}$,
Ra_L Raleigh number based on the characteristic length, $\dfrac{g\cos\gamma_1\beta_T K(T_w - T_\infty)L}{\mu_f \alpha_e}$,
T temperature,
T_w wall temperature,
u tangential velocity,
v normal velocity,

V_w wall mass flux coefficient,
x distance along the cone or the wedge,
y distance normal to the cone or the wedge.

Greek symbols

α_e effective thermal diffusivity of the porous medium, $\frac{\kappa_f}{\rho c_p}$
β_T thermal expansion coefficient,
ϵ viscosity variation parameter,
γ thermal conductivity variation parameter,
γ_1 half angle of the cone or the wedge,
η pesudo-similarity variable,
Γ dimensionless porous medium inertia coefficient,
μ dynamic viscosity,
μ_f dynamic viscosity of the ambient fluid,
θ dimensionless temperature,
ρ density,
ξ dimensionless distance,
ψ stream function.

Subscripts

w condition at the wall,
∞ condition at infinity.

1. Introduction

FLOW AND HEAT transfer from different geometries embedded in porous media have many engineering and geophysical applications such as geothermal reservoirs, drying of porous solids, thermal insulation, enhanced oil recovery, packed-bed catalytic reactors, cooling of nuclear reactors, and underground energy transport. Most early studies on porous media have used the Darcy law, which is a linear empirical relationship between the Darcian velocity and the pressure drop across the porous medium and is limited to slow flows. However, for high velocity flow situations, the Darcy law is inapplicable because it does not account for the resulting inertia effects of the porous medium. In this situation, the relationship between the velocity and the pressure drop is quadratic. The high flow situation is established when the Reynolds number based on the pore size is greater than unity. VAFAI and TIEN [1] have discussed the importance of inertia effects for flows in porous media.

CHENG and MINKOWYCZ [2] have used the Darcy law in their study on free convection about a vertical impermeable flat plate in porous medium. CHENG *et al.* [3] have analyzed the problem of natural convection of a Darcian flow about a cone using the local nonsimilarity method. CHAMKHA [4] has obtained similarity solutions for the problem of non-Darcy free convection from a nonisothermal

cone and a wedge in a porous medium. YIH [5] has reported the effect of uniform lateral mass flux on free convection about a vertical cone embedded in a fluid-saturated porous medium. HOSSAIN *et al.* [6] have studied non-Darcy natural convection heat and mass transfer along a vertical permeable cylinder embedded in a porous medium. YIH [7] studied coupled heat and mass transfer in mixed convection about a wedge embedded in saturated porous medium. CHAMKHA [8] has studied simultaneous heat and mass transfer by natural convection about a vertical wedge and a cone embedded in a porous medium.

In all of the papers mentioned above the viscosity and thermal conductivity are assumed as constant. However, the problem of mixed convection flow past a wedge for temperature-dependent viscosity was investigated by HOSSAIN *et al.* [9]. HASSANIEN [10] analyzed the problem of mixed convection from impermeable vertical wedge in a fluid-saturated porous medium incorporating the variation of permeability and thermal conductivity. HOSSAIN and MUNIR [11] have investigated the natural convection flow of a viscous incompressible fluid from an isothermal truncated cone. HOSSAIN *et al.* [12] have studied the effect of radiation on free convection flow of fluid with variable viscosity from a porous vertical plate.

The aim of the present work is to study the variable viscosity and thermal conductivity effects on heat transfer by natural convection about an isothermal vertical wedge and cone embedded in a fluid-saturated porous medium. A nonsimilarity transformation is employed to transform the governing differential equations to a form whereby they produce their own initial conditions. The transformed equations are solved numerically. The obtained results for special cases of the problem were compared with the previously published work and were found to be in excellent agreement.

2. Problem definition

Consider steady, laminar, heat transfer by natural convection flow over a stationary permeable cone embedded in a fluid-saturated porous medium. Figure 1 shows the schematic diagram of the problem. The origin of the coordinate system is placed at the vertex of the cone, where the x-direction is taken along the cone and the y-direction is normal to the cone. The fluid is assumed to be Newtonian and has constant properties except the density in the buoyancy term of the balance of momentum equation, the viscosity and thermal conductivity. The fluid and the porous medium are assumed to be in local thermal equilibrium. The surface of the cone is kept at constant wall temperature. The temperature at the cone surface is always greater than its uniform ambient values existing far from the cone surface.

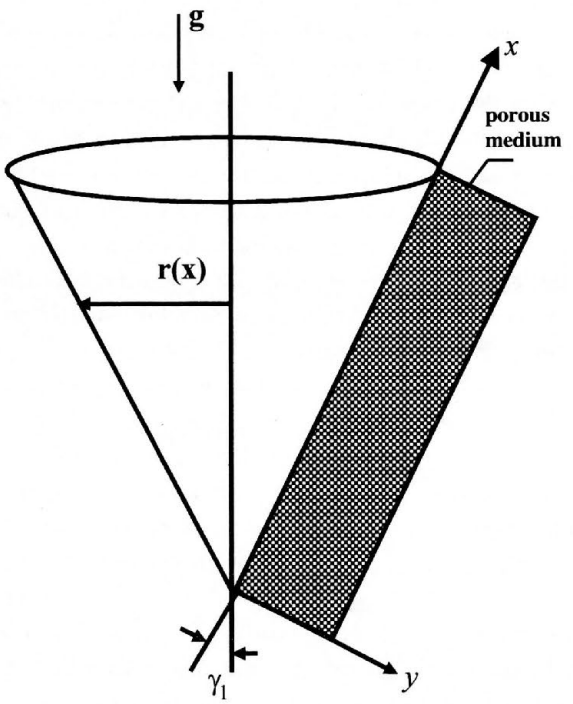

FIG. 1. Flow model and physical coordinate system.

The governing equations that take into account the inertia effects of the porous medium within the boundary layer and Boussinseq approximations may be written as follows:

$$\frac{\partial r^n u}{\partial x} + \frac{\partial r^n v}{\partial y} = 0, \tag{2.1}$$

$$\left[1 + 2\frac{FK}{\mu}u\right]\frac{\partial u}{\partial y} = \mu u \frac{d}{dy}\left(\frac{1}{\mu}\right) + \frac{\rho g \beta_T K \cos\gamma_1}{\mu}\frac{\partial T}{\partial y}, \tag{2.2}$$

$$u\frac{\partial T}{\partial x} + v\frac{\partial T}{\partial y} = \frac{1}{\rho c_p}\frac{\partial}{\partial y}\left(\kappa\frac{\partial T}{\partial y}\right), \tag{2.3}$$

The boundary conditions are defined as follows:

$$v = V_w, \quad T = T_w \quad \text{at} \quad y = 0, \tag{2.4}$$

$$u = 0, \quad T = T_\infty \quad \text{at} \quad y \to \infty, \tag{2.5}$$

where u and v are velocities in the x and y directions, ρ is the density, c_p is the specific heat, g is the gravitational acceleration, K is the permeability of the porous medium, β_T is the thermal expansion coefficient of the fluid, T is the temperature, F is the inertia coefficient of the porous medium, the value V_w (constant) is the surface mass flux coefficient. The value of n can be either $n = 0$ for a flow over a vertical wedge or $n = 1$ for a flow over a vertical cone. When $n = 0$ and $\gamma = 0$, the problem will reduce to the case of a vertical flat plate. The above equations were derived under the assumption that the boundary-layer thickness is sufficiently thin compared to the local radius of the cone. Thus, the local radius at a point in the boundary layer can be replaced by the radius of the cone ($x = r \sin\gamma_1$).

Following [11], the variation of dynamic viscosity and thermal conductivity with the temperature are written in the form:

$$\mu = \mu_f \left[1 + \frac{1}{\mu_f}\left(\frac{d\mu}{dT}\right)_f (T - T_\infty)\right], \tag{2.6}$$

$$\kappa = \kappa_f \left[1 + \frac{1}{\kappa_f}\left(\frac{d\kappa}{dT}\right)_f (T - T_\infty)\right], \tag{2.7}$$

where the subscript f denotes the quantities outside the boundary layers. Introducing the following dimensionless variables:

$$\xi = \frac{2V_w}{\alpha_e \sqrt{\mathrm{Ra}_x}}, \tag{2.8}$$

$$\eta = \frac{y}{x}\sqrt{\mathrm{Ra}_x}, \tag{2.9}$$

$$f(\xi,\eta) = \frac{\psi}{\alpha_e r^n \sqrt{\mathrm{Ra}_x}}, \tag{2.10}$$

$$\theta(\xi,\eta) = \frac{T - T_\infty}{T_w - T_\infty}, \tag{2.11}$$

and substituting Eqs. (2.8)–(2.11) into Eqs. (2.1)–(2.3) we obtain the following transformed governing equations:

$$\left[1 + \frac{\Gamma}{1+\epsilon\theta} f'\right] f'' = \frac{1}{1+\epsilon\theta}\left[-\epsilon f'\theta' + \theta'\right], \tag{2.12}$$

$$[1+\gamma\theta]\,\theta'' + \left(n + \frac{1}{2}\right) f\theta' + \gamma\theta'^2 = \frac{\xi}{2}\left(f'\frac{\partial\theta}{\partial\xi} - \theta'\frac{\partial f}{\partial\xi}\right), \tag{2.13}$$

with the boundary conditions transformed to:

$$f = \frac{\xi}{2n+2}, \quad \theta = 1 \quad \text{at} \quad \eta = 0, \tag{2.14}$$

$$f' = 0, \quad \theta = 0 \quad \text{at} \quad \eta \to \infty, \tag{2.15}$$

where the primes denote partial derivatives with respect to η, $\Gamma = \dfrac{2FK\alpha_e \mathrm{Ra}_L}{\mu_f L}$ is dimensionless porous medium inertia coefficient, $\epsilon = \dfrac{1}{\mu_f}\left(\dfrac{d\mu}{dT}\right)_f (T_w - T_\infty)$ is the viscosity variation parameter, $\gamma = \dfrac{1}{\kappa_f}\left(\dfrac{d\kappa}{dT}\right)_f (T_w - T_\infty)$ is the thermal conductivity variation parameter, and α_e is the equivalent thermal diffusivity. The kind of the applicable fluid for the present form of viscosity and thermal conductivity is discussed in more detail is given in [11, 14]. The velocity components are given by:

$$u = \frac{\alpha_e \mathrm{Ra}_x}{x} f', \tag{2.16}$$

$$v = -\frac{\alpha_e \sqrt{\mathrm{Ra}_x}}{x}\left[(2n+1)f + \xi\frac{\partial f}{\partial \xi} + \eta f'\right]. \tag{2.17}$$

The local Nusselt number Nu_x is given by:

$$\frac{\mathrm{Nu}_x}{\sqrt{\mathrm{Ra}_x}} = -(1+\gamma)\theta'(\xi, 0). \tag{2.18}$$

We now obtain approximate solutions of the equations (2.12)–(2.13) based on the local similarity and non-similarity methods [13]. For the first level of truncation the ξ derivatives in equation (2.13) can be neglected. Thus, the governing equations for the first level of the truncation are equation (2.12) and the following equation:

$$[1+\gamma\theta]\,\theta'' + \left(n + \frac{1}{2}\right) f\theta' + \gamma\theta'^2 = 0 \tag{2.19}$$

subject to the boundary conditions

$$f = -\frac{\xi}{2n+2}, \quad \theta = 1 \quad \text{at} \quad \eta = 0, \tag{2.20}$$

$$f' = 0, \quad \theta = 0 \quad \text{at} \quad \eta \to \infty. \tag{2.21}$$

At the second level of truncation, we introduce $\Pi = \frac{\partial f}{\partial \xi}$, $\Phi = \frac{\partial \theta}{\partial \xi}$ and restore all of neglected terms in the first level of truncation; thus, we have Eq. (2.12) and the following equation:

$$[1+\gamma\theta]\theta'' + \left(n+\frac{1}{2}\right) f\theta' + \gamma\theta'^2 = \frac{\xi}{2}\left(f'\Phi - \theta'\Pi\right) \tag{2.22}$$

subject to the boundary conditions

$$f = \frac{\xi}{2n+2}, \quad \theta = 1 \quad \text{at} \quad \eta = 0, \tag{2.23}$$

$$f' = 0, \quad \theta = 0 \quad \text{at} \quad \eta \to \infty. \tag{2.24}$$

The introduction of the two new dependent variables Π and Φ in the problem requires two equations with appropriate boundary conditions. This can be obtained by differentiating (2.12) and (2.13) with respect to ξ and neglecting the terms $\frac{\partial^2 f}{\partial \xi^2}$ and $\frac{\partial^2 \theta}{\partial \xi^2}$ which leads to

$$\left[1+\frac{\Gamma}{1+\epsilon\theta}\right]\Pi'' - \frac{\epsilon\Gamma}{(1+\epsilon\theta)^2}\Phi f'' = \frac{1}{1+\epsilon\theta}\left[-\epsilon(f'\Phi' + \Pi'\theta') + \Phi'\right] - \frac{\epsilon\Phi}{(1+\epsilon\theta)^2}\left[-\epsilon f'\theta' + \theta'\right], \tag{2.25}$$

$$(1+\gamma\theta)\Phi'' + \gamma\Phi\theta'' + \left(n+\frac{1}{2}\right)(\Pi\theta' + f\Phi') + 2\gamma\theta'\Phi' = \frac{\xi}{2}\left(\Pi\Phi - \Phi'\Pi\right) + \frac{1}{2}\left(f'\Phi - \theta'\Pi\right), \tag{2.26}$$

with boundary conditions

$$\Pi = \frac{1}{2n+2}, \quad \Phi = 0 \quad \text{at} \quad \eta = 0, \tag{2.27}$$

$$\Pi' = 0, \quad \Phi = 0 \quad \text{at} \quad \eta \to \infty. \tag{2.28}$$

The resulting equations with the boundary conditions have been solved numerically using a finite difference method.

3. Results and discussion

Numerical results are obtained for $\epsilon = 0, 5$, $\gamma = 0, 2.5$, $\Gamma = 0, 0.5$, and $n = 0, 1$. In order to verify the accuracy of our present method, we have compared our results with those of YIH [5] and CHAMKHA *et al.* [7]. The present results compared with the above researches are in good agreement, as shown in Table 1. Table 2 gives the parametric conditions for each of the curves shown in Figs. 2–5.

Table 1. Values for $-\theta'(\xi, 0)$ for the cases of wedge $n = 0$ and cone $n = 1$ with ($\Gamma = 0$, $\epsilon = 0$, $\gamma = 0$).

ξ	$n = 0$			$n = 1$		
	YIH [5]	CHAMKHA *et al.* [7]	Present results	YIH [5]	CHAMKHA *et al.* [7]	Present results
−10	4.9999	4.9830	5.0008	5.0995	5.0857	5.1006
−8	3.9999	3.9892	4.0015	4.1244	4.1156	4.1256
−6	2.9999	2.9936	3.0036	3.1655	3.1603	3.1661
−4	2.0015	1.9976	2.0127	2.2434	2.2409	2.2453
−2	1.0725	1.0722	1.0810	1.4139	1.4132	1.4153
0	0.4437	0.4439	0.4445	0.7686	0.7686	0.7687
2	0.1416	0.1423	0.1355	0.3537	0.3541	0.3530
4	0.0333	0.0340	0.0229	0.1342	0.1349	0.1309
6	0.0055	0.0058	0.0011	0.0400	0.0411	0.03559
8	0.0006	0.0007	0.000009	0.0092	0.0096	0.0064
10	0.0001	0.0001	0.0	0.0016	0.0017	0.0006

Table 2. Parametric values for curves in the figures.

Curve	Γ	ϵ	γ
I	0	0	0
II	0.5	0	0
III	0	0	2.5
IV	0.5	0	2.5
V	0	5	2.5
VI	0.5	5	2.5

Figures 2 and 3 represent the behavior of the stream function and the fluid velocity for the situations shown in Table 2 for both a cone and a wedge at positive lateral wall mass flux at $\xi = 10$. A resistance against the flow exists if the porous medium inertia effect is considered. As a result, the flow stream function and velocities near the wall decrease as shown by curves II and IV compared with curves I and III for a cone and a wedge. Also, the effect of viscosity and

thermal conductivity variation parameters on both the stream function and the velocity is observed. It is found that the flow stream functions and velocities near the wall decrease as the viscosity variation parameter ϵ or thermal conductivity variation parameter γ increase.

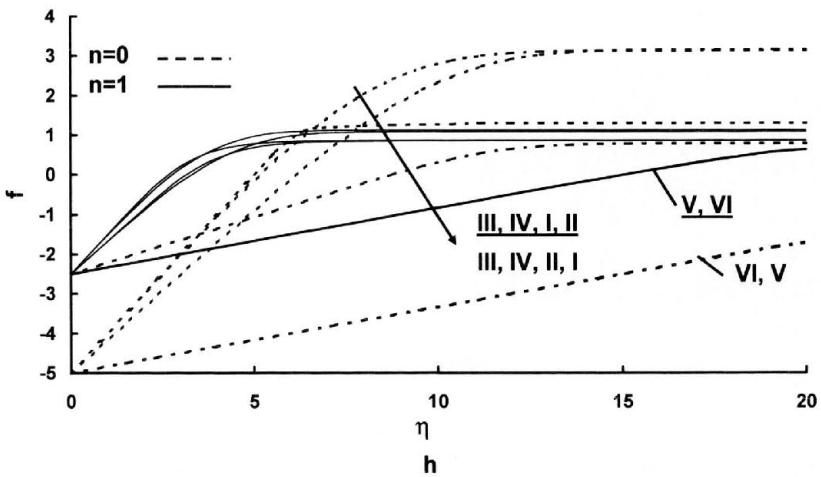

FIG. 2. Stream function distribution for various values of ϵ, γ and n.

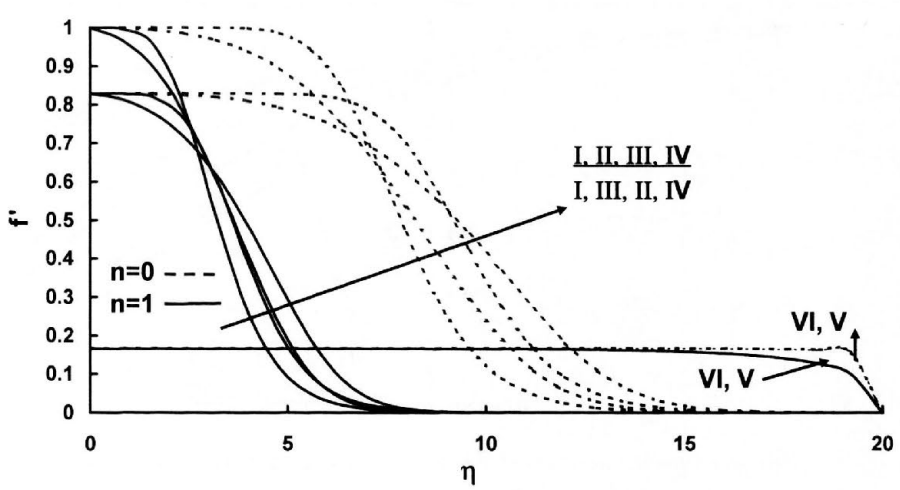

FIG. 3. Velocity distribution for various values of ϵ, γ and n.

Figure 4 illustrates the temperature profiles for a cone and a wedge at $\xi = 10$. The resistive force discussed in the previous paragraph due to the presence of inertia effect tends to increase the temperature of the flow for a wedge and a cone.

It is also seen that the temperature increases as viscosity variation parameter. Also, as thermal conductivity variation parameter increases, the temperature profiles decrease near the wall.

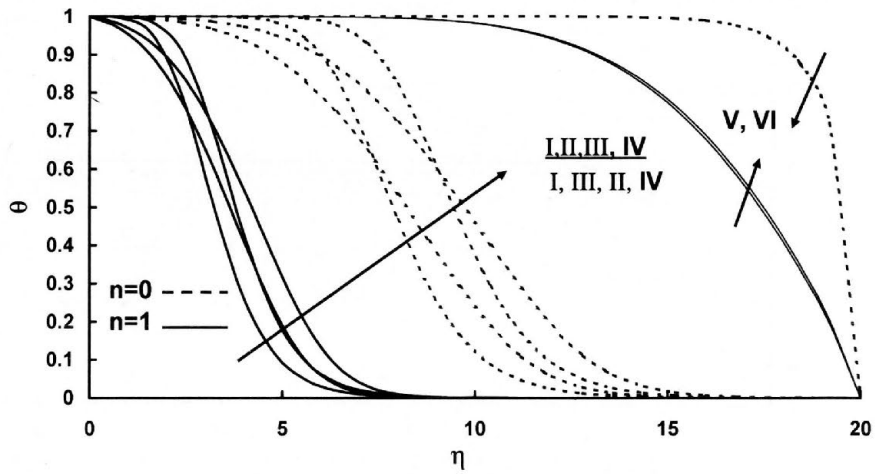

FIG. 4. Temperature distribution for various values of ϵ,γ and n.

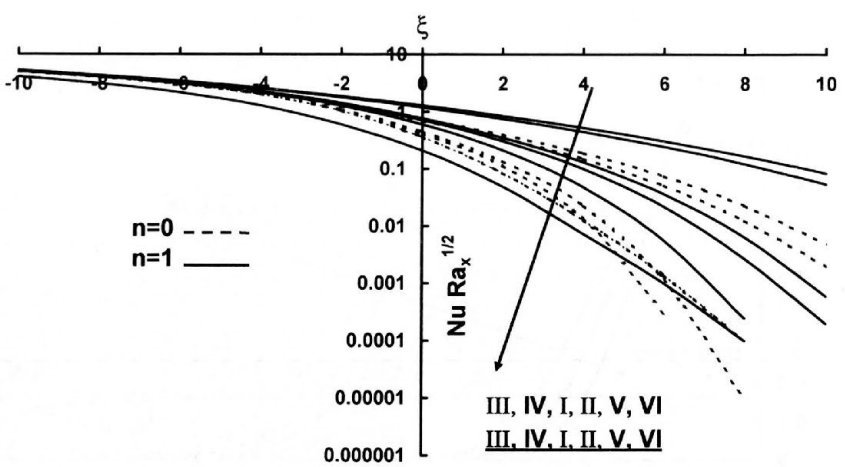

FIG. 5. Nusselt number distribution for various values of ϵ, γ and n.

Figure 5 illustrates the distribution of the local Nusselt number for a wedge and a cone. The porous medium inertia effect tends to decrease the local Nusselt number due to its effect on the wall temperature slopes. As viscosity variation parameter increases, the Nusselt number decreases. On the contrary, the Nusselt number increases as thermal conductivity variation parameter γ increases.

4. Conclusions

The problem of steady, laminar heat transfer by natural convection boundary layer flow of variable viscosity and thermal conductivity over an isothermal vertical permeable cone or wedge with constant lateral wall mass flux embedded in a uniform porous medium was considered. The governing equations for uniform wall temperature were developed and transformed by using appropriate nonsimilarity transformations. The transformed equations were solved numerically by using the Keller-Box method. The numerical results are presented. It is found that the Nusselt number decreased when the porous medium inertia or thermal conductivity variation parameter effects are considered. Furthermore, the local Nusselt number increases in the presence of the viscosity variation parameter.

References

1. K. VAFAI, C. L. TIEN, *Boundary and inertia effects on flow and heat transfer in porous media*, Int. J. Heat Mass Transfer, **24**, 195–203, 1981.
2. P. CHENG, W. J. MINKOWYCZ, *Free convection about a vertical flat plate embedded in a porous medium with application to heat transfer from a dike*, J. Geophys. **82**, 2040–2044, 1977.
3. P. CHENG, T. LE, I. POP, *Natural convection of a Darcian fluid about a cone*, Int. Commun. Heat Mass Transfer, **12**, 705–717, 1985.
4. A. J. CHAMKHA, *Non-Darcy hydromagnetic free convection from a cone and a wedge in porous media*, Int. Comm. Heat Mass Transfer, **23**, 875-887, 1996.
5. K. A. YIH, *The effect of uniform lateral mass flux on free convection about a vertical cone embedded in a porous media*, Int. Commun. Heat Mass Transfer, **24**, 1195–1205, 1997.
6. M. A. HOSSAIN, K. VAFAI, K. KHANAFER, *Non-Darcy natural convection heat and mass transfer along a vertical permeable cylinder embedded in a porous medium*, Int. J. Thermal Sci., **38**, 854–862, 1999.
7. K. A. YIH, *Coupled heat and mass transfer in mixed convection over a VHF/VMF wedge in porous media: the entire regime*, Acta Mechanica, **137**, 1–12, 1999.
8. A. J. CHAMKHA, A. R. A. KHALED, O. AL-HAWAJ, *Simultaneous heat and mass transfer by natural convection from a cone and a wedge in porous media*, J. Porous Media, **3**, 155–164, 2000.
9. M. A. HOSSAIN, M. S. MUNIR, D. A. S. REES, *Flow of viscous incompressible fluid with temperature-dependent viscosity and thermal conductivity past a permeable wedge with uniform surface heat flux*, Int. J. Thermal Sci., **39**, 635–644, 2000.
10. I. A. HASSANIEN, *Variable permeability effects on mixed convection along a vertical wedge embedded in a porous medium with variable surface heat flux*, Applied Mathematics and Computation, **138**, 41–59, 2003.
11. M. A. HOSSAIN, M. S. MUNIR, *Natural convection flow of a viscous fluid about a truncated cone with temperature-dependent viscosity and thermal conductivity*, Int. J. Num. Methods. Heat Fluid Flow, **11**, 494–510, 2001.

12. M. A. HOSSAIN, K. KHANAFER, K. VAFAI, *The effect of radiation on free convection flow of fluid with variable viscosity from a porous vertical plate,* Int. J. Thermal Sci. **40**, 115–124, 2001.

13. E. M. SPARROW, H. QUACK, J. BOERNER, *Local non-similarity boundary solutions,* AIAA, **8**, 1936–1942, 1970.

14. P. L. GELRINGER, *Hand book of heat transfer medium*, New York 1962.

Received February 28, 2002; revised version June 6, 2003.

Arch. Mech., **55**, 4, pp. 357–371, Warszawa 2003

Analytical expressions of effective constants for a piezoelectric composite reinforced with square cross-section fibers

J. A. OTERO[(1)], J. BRAVO-CASTILLERO[(2)], R. GUINOVART-DÍAZ[(2)], R. RODRÍGUEZ-RAMOS[(2)], G. A. MAUGIN[(3)]

[(1)] *Instituto de Cibernética, Matemática y Física*
Calle 15 e/t C y D,
C.P. 10400, Vedado, La Habana, Cuba

[(2)] *Facultad de Matemática y Computación Universidad de la Habana,*
San Lázaro y L, Vedado, C.P. 10400,
Vedado, La Habana, Cuba

[(3)] *Laboratoire de Modélisation en Mécanique,*
Université Pierre et Marie Curie. Case 162, 8 rue du Capitaine Scott.
75015 Paris, France

THE PURPOSE of this paper is to present analytical expressions of the effective elastic, piezoelectric and dielectric constants of reinforced piezoelectric composite materials with unidirectional fibers periodically distributed in a square matrix, as obtained by means of the "double asymptotic homogenization" method. The cross-section of the fibers is square. Each periodic cell of the medium is a binary piezoelectric composite wherein both phases are homogeneous piezoelectric materials with transversely isotropic properties. Comparison between the derived theoretical predictions of characteristic parameters and the existing experimental results shows a rather good agreement. The results obtained in the present paper were verified by means of the universal relations of Schulgasser. Numerical computation of the effective properties can be realized without difficulties.

Key words: Piezocomposite, effective properties, asymptotic homogenization, fiber-reinforced, composite material.

1. Introduction

The piezocomposite materials have been used for hydrophone applications and transducers for medical imaging. The determination of the overall properties of piezocomposite, according to the physical and geometric characteristics of their components, is very important for applications.

Different techniques have been reported to estimate the effective electroelastic properties of piezoelectric laminate composites. For example, in [1] the effective coefficients of a bi-laminate medium of 4mm symmetry using the hy-

potheses of equivalent homogeneity were obtained. In [2], the effective behavior of bi-laminate media of hexagonal symmetry using the theory of uniform fields in heterogeneous media by means of appropriate boundary conditions was determined. An effective medium model of layered composites has been investigated starting from a physical reasoning given in [3]. In the case of very fine composite structures, quasistatic and iso-strain (constant strain) approximations were used to derive the effective properties of composites (see, [4, 5]) which include the effective elasticity, permittivity, piezoelectricity, and density; some physical parameters useful for different applications were derived. Basing on the asymptotic homogenization method, analytical formulae for the overall properties of layered piezoelectric composites can be found in [6, 7].

Unidirectional fibrous composite with square cross-sections of fibers has been investigated only by means of numerical solution of the local problems. For instance, the finite element method was applied in [8] for determine the global properties of a piezocomposite. The Ritz method was used in [6] to investigate a rectangular cross-section in a square matrix for thermopiezoelectric composites.

In the present paper, using "double homogenization", (e.g., the homogenization is applied two times in different directions, according to the geometric configuration of the composite), analytical expressions of the effective coefficients are obtained, in a composite with square fibers distributed periodically into square cells. Somehow, the present work is related to a recent work by ANDRIANOV *et al.* [9, 10], where an asymptotic approach and Padé approximants are proposed for evaluating effective elastic and heat conductivity properties respectively, of two-component periodic composites with fibrous inclusions. In order to apply the so-called "double homogenization", the problem is divided into two homogenization stages: 1) the composite structure is homogenized, that is, the effective coefficients for a unidirectional structure in the direction x_2 are obtained; 2) afterwards, the effective coefficients are calculated for the composite 2–2 in the other direction x_1. In this case, due to the symmetry of the composite, the double homogenization can be easily realized. The main theoretical aspects used in this work can be found in [7]. These results for square fibers are compared with the expressions obtained in [7] for the laminate composites 2–2, and with some theoretical and experimental results reported in the literature, [11]. The universal relations given in [12] are satisfied for the set of coefficients calculated in the present work.

2. Theoretical procedure

Piezoelectric materials are characterized by the following different material coefficients: C (elastic), e (piezoelectric) and ε (dielectric), which are the fourth, third and second order tensors, respectively. When these materials are hetero-

geneous and periodic, the material coefficients are X-periodic functions. Here X denotes the periodic cell. Applying the method of asymptotic homogenization, the material coefficients are transformed into new physical coefficients $\overline{C}$ (elastic), $\overline{e}$ (piezoelectric) and $\overline{\varepsilon}$ (dielectric), which represent the homogeneous properties or effective coefficients. To obtain these coefficients it is necessary to solve a set of local problems, which are represented by a system of partial differential equations. In case of circular transverse section of fibers, an analytical solution for this system is obtained making use of the potential methods of the complex variable and properties of the Weierstrass elliptic functions, [13–17]. On the other hand, analytical closed forms of the effective coefficients of piezoelectric composites with square transverse sections of the fibers using asymptotic homogenization have not been reported yet. Therefore the purpose of the present work is to present an alternative form for the computation of analytical expressions for such composites.

Let us suppose that we have a composite material with unidirectional square fibers periodically distributed, where each periodic cell is a binary homogeneous piezoelectric medium with square symmetry in welded contact at the interface. Both the matrix and the fibers are assumed to be composed of homogeneous piezoelectric materials with 6 mm hexagonal symmetry.

2.1. Effective coefficients for the first homogenization in the direction x_2

In [7], the effective coefficients were obtained for piezoelectric laminated composites. Let us suppose that we have a laminate material formed by a piezoelectric phase (phase 1) of elastic, piezoelectric, dielectric and density constants $C_{ij}^{(1)}$, $e_{ij}^{(1)}$, $\varepsilon_{ij}^{(1)}$, $\rho^{(1)}$ respectively; and a phase of piezoelectric polymer (phase 2) of elastic, piezoelectric, dielectric and density parameters denoted by: $C_{ij}^{(2)}$, $e_{ij}^{(2)}$, $\varepsilon_{ij}^{(2)}$, $\rho^{(2)}$.

The effective coefficients for a piezoelectric laminate in the direction x_2 are exactly expressed as follows:

Effective elastic constants

$$C_{11}^{*} = -\frac{\Gamma_L^2\alpha_{12} + \Gamma_L(-C_{11}^{(1)}\beta_{12} - \alpha_{12} + C_{11}^{(2)}\beta_{12}) - C_{11}^{(2)}\beta_{12}}{\beta_{12}},$$

$$C_{12}^{*} = -\frac{(C_{12}^{(1)} - C_{12}^{(2)})C_{22}^{(1)}(\Gamma_L - 1) - C_{12}^{(1)}\beta_{12}}{\beta_{12}}, \tag{2.1}$$

$$C_{13}^{*} = -\frac{\Gamma_L^2\alpha_2^{(2)} + \Gamma_L(-C_{13}^{(1)}\beta_{12} - \alpha_{22} + C_{13}^{(2)}\beta_{12}) - C_{13}^{(2)}\beta_{12}}{\beta_{12}},$$

(2.1) [cont.]

$$C_{22}^{*} = -\frac{C_{22}^{(1)}C_{22}^{(2)}}{\beta_{12}},$$

$$C_{23}^{*} = -\frac{(C_{23}^{(1)} - C_{23}^{(2)})C_{22}^{(1)}(\Gamma_L - 1) - C_{23}^{(1)}\beta_{12}}{\beta_{12}},$$

$$C_{33}^{*} = -\frac{\Gamma_L^2\alpha_{32} + \Gamma_L(-C_{33}^{(1)}\beta_{12} - \alpha_{32} + C_{33}^{(2)}\beta_{12}) - C_{33}^{(2)}\beta_{12}}{\beta_{12}},$$

$$C_{44}^{*} = \frac{-2.\varepsilon_{22}^{(2)}\Gamma_L\left(e_{24}^{(1)}e_{24}^{(2)}\right)^2\beta_{32}\beta_{42} + (2.\varepsilon_{22}^{(2)}\Gamma_L\beta_{32}\beta_{42} + \beta_{32}(\beta_{42})^2)\left(e_{24}^{(2)}\right)^4}{\beta_{32}\varepsilon_{22}^{(1)}\varepsilon_{22}^{(2)}\beta_{42}}$$

$$+ \frac{\varepsilon_{22}^{(2)}\Gamma_L\left(e_{24}^{(1)}\right)^2\beta_{32}\beta_{42} - \left(C_{44}^{(1)}\varepsilon_{22}^{(2)}\right)^2\varepsilon_{22}^{(1)} - C_{44}^{(1)}\varepsilon_{22}^{(1)}\left(\varepsilon_{22}^{(2)}\right)^2\beta_{32}}{\beta_{32}\varepsilon_{22}^{(1)}\varepsilon_{22}^{(2)}\beta_{42}}$$

$$+ \frac{(-\beta_{32}(\beta_{42})^2 - \varepsilon_{22}^{(2)}\Gamma_L\beta_{32}\beta_{42})\left(e_{24}^{(2)}\right)^2 C_{44}^{(1)}C_{44}^{(2)}\left(\varepsilon_{22}^{(1)}\right)^2\varepsilon_{22}^{(2)}}{\beta_{32}\varepsilon_{22}^{(1)}\varepsilon_{22}^{(2)}\beta_{42}}$$

$$+ \frac{\Gamma_L^2\left(\varepsilon_{22}^{(2)}\right)^2\beta_{32}\alpha_{42} + C_{22}^{(1)}\left(\varepsilon_{22}^{(1)}\right)^2\varepsilon_{22}^{(2)}\beta_{32} - \left(C_{44}^{(1)}\right)^2\beta_{42}\varepsilon_{22}^{(2)}\varepsilon_{22}^{(1)}}{\beta_{32}\varepsilon_{22}^{(1)}\varepsilon_{22}^{(2)}\beta_{42}},$$

$$C_{55}^{*} = C_{55}^{(1)}\Gamma_L + C_{55}^{(2)} - C_{55}^{(2)}\Gamma_L,$$

$$C_{66}^{*} = \frac{1}{2}\frac{(C_{22}^{(1)} - C_{12}^{(1)})(C_{22}^{(2)} - C_{12}^{(2)})}{\beta_{22} - \beta_{12}}.$$

Effective piezoelectric constants

(2.2)

$$e_{24}^{*} = \frac{(-e_{24}^{(1)} + e_{24}^{(2)})\varepsilon_{22}^{(2)}\Gamma_L + e_{24}^{(2)}\beta_{42}}{\beta_{42}},$$

$$e_{32}^{*} = -\frac{(e_{32}^{(1)} - e_{32}^{(2)})C_{22}^{(1)}\Gamma_L + (-e_{32}^{(1)} + e_{32}^{(2)})C_{22}^{(1)} - e_{32}^{(1)}\beta_{12}}{\beta_{12}},$$

$$e_{15}^{*} = e_{15}^{(1)}\Gamma_L + e_{15}^{(2)} - e_{15}^{(2)}\Gamma_L,$$

$$e_{33}^{*} = -\frac{\Gamma_L e_{33}^{(2)}\beta_{12} - \Gamma_L\alpha_{52} - \Gamma_L e_{33}^{(1)}\beta_{12} + \Gamma_L^2\alpha_{52} - e_{33}^{(2)}\beta_{12}}{\beta_{12}},$$

$$e_{31}^{*} = -\frac{-e_{31}^{(2)}\beta_{12} + \Gamma_L^2\alpha_{72} - \Gamma_L\alpha_{72} - \Gamma_L e_{31}^{(x_1)}\beta_{12} + \Gamma_L e_{31}^{(2)}\beta_{12}}{\beta_{12}}.$$

Effective dielectric constants

$$\varepsilon_{11}^{*} = \varepsilon_{11}^{(1)}\Gamma_L + \varepsilon_{11}^{(2)} - \varepsilon_{11}^{(2)}\Gamma_L,$$

$$\varepsilon_{33}^{*} = \frac{-\Gamma_L\varepsilon_{33}^{(2)}\beta_{12} + \Gamma_L\varepsilon_{33}^{(1)}\beta_{12} - \Gamma_L^2\alpha_{72} + \varepsilon_{33}^{(2)}\beta_{12} + \Gamma_L\alpha_{72}}{\beta_{12}}, \tag{2.3}$$

$$\varepsilon_{22}^{*} = -\frac{\varepsilon_{22}^{(1)}\varepsilon_{22}^{(2)}}{\beta_{42}}.$$

Effective density constant

$$\rho^{*} = \rho^{(1)}\Gamma_L + \rho^{(2)} - \rho^{(2)}\Gamma_L. \tag{2.4}$$

where

$$\beta_{12} = -\Gamma_L C_{22}^{(2)} - C_{22}^{(1)} + C_{22}^{(1)}\Gamma_L,$$

$$\beta_{22} = -\Gamma_L C_{12}^{(2)} - C_{12}^{(1)} + C_{12}^{(1)}\Gamma_L,$$

$$\beta_{32} = -\Gamma_L C_{44}^{(1)} + C_{44}^{(2)} - C_{44}^{(2)}\Gamma_L,$$

$$\beta_{42} = -\Gamma_L\varepsilon_{22}^{(2)} - \varepsilon_{22}^{(1)} + \varepsilon_{22}^{(1)}\Gamma_L,$$

$$\alpha_{12} = (C_{12}^{(1)} - C_{12}^{(2)})(C_{12}^{(1)} - C_{12}^{(2)}),$$

$$\alpha_{22} = (C_{12}^{(1)} - C_{12}^{(2)})(C_{23}^{(1)} - C_{23}^{(2)}),$$

$$\alpha_{32} = (C_{23}^{(1)} - C_{23}^{(2)})(C_{23}^{(1)} - C_{23}^{(2)}),$$

$$\alpha_{42} = (e_{24}^{(1)} - e_{24}^{(2)})(e_{24}^{(1)} - e_{24}^{(2)}),$$

$$\alpha_{52} = (C_{23}^{(1)} - C_{23}^{(2)})(e_{32}^{(1)} - e_{32}^{(2)}),$$

$$\alpha_{62} = (C_{12}^{(1)} - C_{12}^{(2)})(e_{32}^{(1)} - e_{32}^{(2)}),$$

$$\alpha_{72} = -(e_{32}^{(1)} - e_{32}^{(2)})(e_{32}^{(1)} - e_{32}^{(2)}).$$

The expressions C_{ij}^{*}, e_{ij}^{*}, ε_{ij}^{*} and ρ^{*} represent the effective coefficients in the Structure I (Fig. 1) and we denote by Γ_L the volume fraction of piezoelectric material in this structure.

2.2. Effective coefficients for the second homogenization in the direction x_1

Now, the laminated composite is made of Phase 1 whose properties are the averaged coefficients in the direction x_2 calculated previously, namely: C_{ij}^{*}, e_{ij}^{*}, ε_{ij}^{*}, ρ^{*} and a phase of piezoelectric polymer (Phase 2) of elastic, piezoelectric, dielectric and density properties denoted by: $C_{ij}^{(2)}$, $e_{ij}^{(2)}$, $\varepsilon_{ij}^{(2)}$, $\rho^{(2)}$.

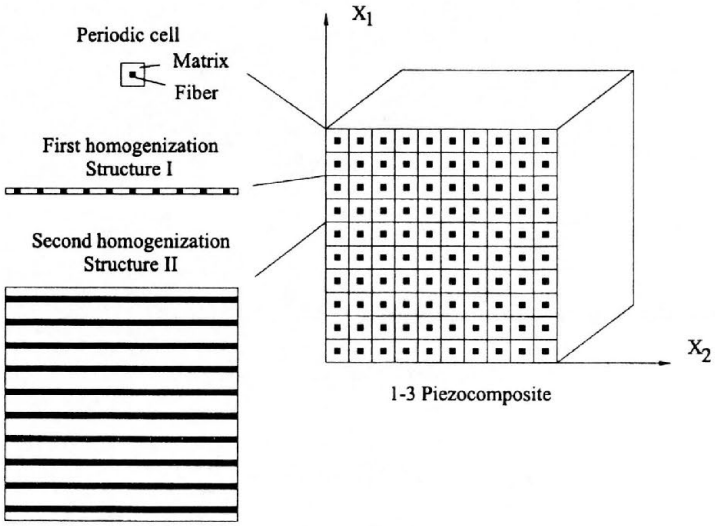

FIG. 1. Schematic diagram of a 1–3 piezoelectric composite, illustrating the periodic cell and two homogenization stages.

The effective coefficients of the composite in the direction x_1 are exactly given in the following form:

Effective elastic constants

$$
\begin{aligned}
\overline{C}_{11} &= -\frac{C^*_{11}C^{(2)}_{11}}{\beta_{11}},\\
\overline{C}_{12} &= -\frac{(C^*_{12}-C^{(2)}_{12})C^*_{11}(\Gamma_L-1)-C^*_{12}\beta_{11}}{\beta_{11}},\\
\overline{C}_{13} &= -\frac{(C^*_{13}-C^{(2)}_{13})C^*_{11}(\Gamma_L-1)-C^*_{13}\beta_{11}}{\beta_{11}},\\
\overline{C}_{22} &= -\frac{\Gamma_L^2\alpha_{11}+\Gamma_L(-C^*_{22}\beta_{11}-\alpha_{11}+C^{(2)}_{22}\beta_{11})-C^{(2)}_{22}\beta_{11}}{\beta_{11}},\\
\overline{C}_{23} &= -\frac{\Gamma_L^2\alpha_{21}+\Gamma_L(-C^*_{23}\beta_{11}-\alpha_{21}+C^{(2)}_{23}\beta_{11})-C^{(2)}_{23}\beta_{11}}{\beta_{11}},\\
\overline{C}_{33} &= -\frac{\Gamma_L^2\alpha_{31}+\Gamma_L(-C^*_{33}\beta_{11}-\alpha_{31}+C^{(2)}_{33}\beta_{11})-C^{(2)}_{33}\beta_{11}}{\beta_{11}},\\
\overline{C}_{44} &= C^*_{44}\Gamma_L+C^{(2)}_{44}-C^{(2)}_{44}\Gamma_L,
\end{aligned}
\tag{2.5}
$$

(2.5) [cont.]
$$\overline{C}_{55} = \frac{-2.\varepsilon_{11}^{(2)}\Gamma_L\left(e_{15}^{*}e_{15}^{(2)}\right)^2\beta_{31}\beta_{41} + (2.\varepsilon_{11}^{(2)}\Gamma_L\beta_{31}\beta_{41} + \beta_{31}\beta_{41}^2)\left(e_{15}^{(2)}\right)^4}{\beta_{31}\varepsilon_{11}^{*}\varepsilon_{11}^{(2)}\beta_{41}}$$
$$+ \frac{\varepsilon_{11}^{(2)}\Gamma_L(e_{15}^{*})^2\beta_{31}\beta_{41} - \left(C_{55}^{*}\varepsilon_{11}^{(2)}\right)^2\varepsilon_{11}^{*} - C_{55}^{*}\varepsilon_{11}^{*}\left(\varepsilon_{11}^{(2)}\right)^2\beta_{31}}{\beta_{31}\varepsilon_{11}^{*}\varepsilon_{11}^{(2)}\beta_{41}}$$
$$+ \frac{(-\beta_{31}\beta_{41}^2 - \varepsilon_{11}^{(2)}\Gamma_L\beta_{31}\beta_{41})\left(e_{15}^{(2)}\right)^2 C_{55}^{*}C_{55}^{(2)}(\varepsilon_{11}^{*})^2\varepsilon_{11}^{(2)}}{\beta_{31}\varepsilon_{11}^{*}\varepsilon_{11}^{(2)}\beta_{41}}$$
$$+ \frac{\Gamma_L^2\left(\varepsilon_{11}^{(2)}\right)^2\beta_{31}\alpha_{41} + C_{55}^{*}(\varepsilon_{11}^{*})^2\varepsilon_{11}^{(2)}\beta_{31} - (C_{55}^{*})^2\beta_{41}\varepsilon_{11}^{(2)}\varepsilon_{11}^{*}}{\beta_{31}\varepsilon_{11}^{*}\varepsilon_{11}^{(2)}\beta_{41}},$$

$$\overline{C}_{66} = \frac{1}{2}\frac{(C_{11}^{*} - C_{12}^{*})(C_{11}^{(2)} - C_{12}^{(2)})}{\beta_{21} - \beta_{11}},$$

Effective piezoelectric constants

$$\overline{e}_{15} = \frac{(-e_{15}^{*} + e_{15}^{(2)})\varepsilon_{11}^2\Gamma_L + e_{15}^{(2)}\beta_{41}}{\beta_{41}},$$

$$\overline{e}_{31} = -\frac{(e_{31}^{*} - e_{31}^{(2)})C_{11}^{*}\Gamma_L + (-e_{31}^{*} + e_{31}^{(2)})C_{11}^{*} - e_{31}^{*}\beta_{11}}{\beta_{11}},$$

(2.6)
$$\overline{e}_{24} = e_{24}^{*}\Gamma_L + e_{24}^{(2)} - e_{24}^{(2)}\Gamma_L,$$

$$\overline{e}_{33} = -\frac{\Gamma_L e_{33}^{(2)}\beta_{11} - \Gamma_L\alpha_{51} - \Gamma_L e_{33}^{*}\beta_{11} + \Gamma_L^2\alpha_{51} - e_{33}^{(2)}\beta_{11}}{\beta_{11}},$$

$$\overline{e}_{32} = -\frac{-e_{32}^{(2)}\beta_{11} + \Gamma_L^2\alpha_{71} - \Gamma_L\alpha_{71} - \Gamma_L e_{32}^{*}\beta_{11} + \Gamma_L e_{32}^{(2)}\beta_{11}}{\beta_{11}}.$$

Effective dielectric constants

$$\overline{\varepsilon}_{22} = \varepsilon_{22}^{*}\Gamma_L + \varepsilon_{22}^{(2)} - \varepsilon_{22}^{(2)}\Gamma_L,$$

(2.7)
$$\overline{\varepsilon}_{33} = \frac{-\Gamma_L\varepsilon_{33}^{(2)}\beta_{11} + \Gamma_L\varepsilon_{33}^{*}\beta_{11} - \Gamma_L^2\alpha_{71} + \varepsilon_{33}^{(2)}\beta_{11} + \Gamma_L\alpha_{71}}{\beta_{11}},$$

$$\overline{\varepsilon}_{11} = -\frac{\varepsilon_{11}^{*}\varepsilon_{11}^{(2)}}{\beta_{41}}.$$

Effective density constant

(2.8)
$$\overline{\rho} = \rho^{*}\Gamma_L + \rho^{(2)} - \rho^{(2)}\Gamma_L,$$

where

$$\begin{aligned}
\beta_{11} &= -\Gamma_L C_{11}^{(2)} - C_{11}^* + C_{11}^* \Gamma_L, \\
\beta_{21} &= -\Gamma_L C_{12}^{(2)} - C_{12}^* + C_{12}^* \Gamma_L, \\
\beta_{31} &= -\Gamma_L C_{55}^* + C_{55}^{(2)} - C_{55}^{(2)} \Gamma_L, \\
\beta_{41} &= -\Gamma_L \varepsilon_{11}^{(2)} - \varepsilon_{11}^* + \varepsilon_{11}^* \Gamma_L, \\
\alpha_{11} &= (C_{12}^* - C_{12}^{(2)})(C_{12}^* - C_{12}^{(2)}), \\
\alpha_{21} &= (C_{12}^* - C_{12}^{(2)})(C_{13}^* - C_{13}^{(2)}), \\
\alpha_{31} &= (C_{13}^* - C_{13}^{(2)})(C_{13}^* - C_{13}^{(2)}), \\
\alpha_{41} &= (e_{15}^* - e_{15}^{(2)})(e_{15}^* - e_{15}^{(2)}), \\
\alpha_{51} &= (C_{13}^* - C_{13}^{(2)})(e_{31}^* - e_{31}^{(2)}), \\
\alpha_{61} &= (C_{12}^* - C_{12}^{(2)})(e_{31}^* - e_{31}^{(2)}), \\
\alpha_{71} &= -(e_{31}^* - e_{31}^{(2)})(e_{31}^* - e_{31}^{(2)}).
\end{aligned}$$

The expressions $\overline{C}_{ij}$, $\overline{e}_{ij}$, $\overline{\varepsilon}_{ij}$ and $\overline{\rho}$ denote the effective coefficients in the composite Structure II. These expressions represent the effective coefficients of the composite for square reinforcement fibers. The volume fraction of fibers is expressed according to $\Gamma_F = (\Gamma_L)^2$.

3. Applications to transducers. Results

One of the important applications of the piezoelectric composite materials appears in transducers used for medical imaging applications. The desired properties are a high electromechanical coupling coefficient K_t (0.6 to 0.7) and a low acoustic impedance Z (< 7.5 MRayls). Now, the case in which two different homogeneous phases are involved in the composite is studied. The effective properties of the composite can now be computed from Eqs. (2.5)–(2.8). A set of important physical parameters for pulse-echo transducer applications can be calculated. For instance, let us mention the electromechanical piezoelectric coupling coefficients K_t and K_p, the specific acoustic impedance Z, the longitudinal wave speed V_l and the hydrostatic charge coefficient d_h. They are given by the following formulae (see, [18]):

$$\overline{K}_t = \sqrt{1 - \frac{\overline{C}_{33}}{\overline{C}_{33}^D}}, \tag{3.1}$$

$$\overline{K}_p = \sqrt{\frac{2}{1-\overline{\sigma}}}\overline{K}_{31},$$

$$\overline{Z} = \overline{\rho}\overline{V}_3^D,$$

(3.1) [cont.]

$$\overline{V}_l = \sqrt{\frac{\overline{C}_{33}^D}{\overline{\rho}}},$$

$$\overline{d}_h = \overline{d}_{31} + \overline{d}_{32} + \overline{d}_{33},$$

where

$$\overline{C}_{33}^D = \overline{C}_{33} + \overline{e}_{33}^2(\overline{\varepsilon}_{33})^{-1},$$

$$\overline{K}_{31} = \frac{\overline{d}_{31}}{\sqrt{\overline{\varepsilon}_{33}^T\overline{S}_{11}}},$$

(3.2)

$$\overline{\sigma} = -\frac{\overline{S}_{12}}{\overline{S}_{11}},$$

$$\overline{S}_{ij} = (-1)^{i+j}\frac{\triangle_{ij}}{\triangle},$$

$$\overline{d}_{mi} = \overline{e}_{mj}\overline{S}_{ji},$$

$$\overline{\varepsilon}_{mn}^T = \overline{d}_{mp}\overline{e}_{np} + \overline{\varepsilon}_{mn}$$

The superscripts D and T at a given symbol in (3.1) and (3.2) mean that the relevant quantity is measured at constant electric displacement D or at constant stress T; $\overline{d}_{ij}$ is the piezoelectric coefficient of the composite, $\overline{S}_{ij}$ are components of the effective compliance tensor $\overline{S}$, $\overline{\sigma}$ is the Poisson's ratio, $\triangle$ is determinant of the $\overline{C}_{ij}$ matrix and $\triangle_{ij}$ is the minor obtained by excluding the i-th row and j-th column. Some properties of the composite are presented as functions of the volume fraction of piezoelectric phase and also their implications for the design of pulse-echo ultrasonic transducers are shown. Material parameters of the piezoelectric and polymer phases used in the calculations are shown in Table 1.

A composite of $PZT - 5A$ rods embedded in a passive polymer Araldite is now considered. The material values appearing in Table 1 were taken from [7, 11]. In Fig. 2, the electromechanical piezoelectric coupling coefficients $\overline{K}_t$ and $\overline{K}_p$ are plotted as functions of the piezoelectric volume fraction. The dotted line corresponds to the laminated composite 2–2 and the solid line to the fibrous composite 1–3. We observe that the value of $\overline{K}_t$ for the fibrous composite is greater than that for the laminated composite. Also we can appreciate that

for the same values of piezoelectric volume fraction, the 1–3 composite has a smaller value of $\overline{K}_p$. Therefore, the composite 1–3 has better physical properties than the composite 2–2 for applications in transducers used for medical imaging applications.

Table 1. Material parameters

	PZT 5A	ARALDITE	TLZ-5	VDF/TrFE copolymer
C_{11}^E (10^{10}N/m^2)	12.10	0.546	12.6	0.85
C_{12}^E (10^{10}N/m^2)	7.54	0.294	7.95	0.36
C_{13}^E (10^{10}N/m^2)	7.52	0.294	8.41	0.36
C_{33}^E (10^{10}N/m^2)	11.10	0.546	10.9	0.99
e_{33} (C/m^2)	15.8	–	24.8	−0.29
e_{31} (C/m^2)	−5.4	–	−6.5	0.008
$\varepsilon_{33}^S/\varepsilon_0$	916	7.0	1813	6.0
ρ (10^3Kg/m^3)	7.75	1.17	7.898	1.88

$\varepsilon_0 = 8.85\ 10^{-12}$ C^2/Nm^2 (permittivity of free space)

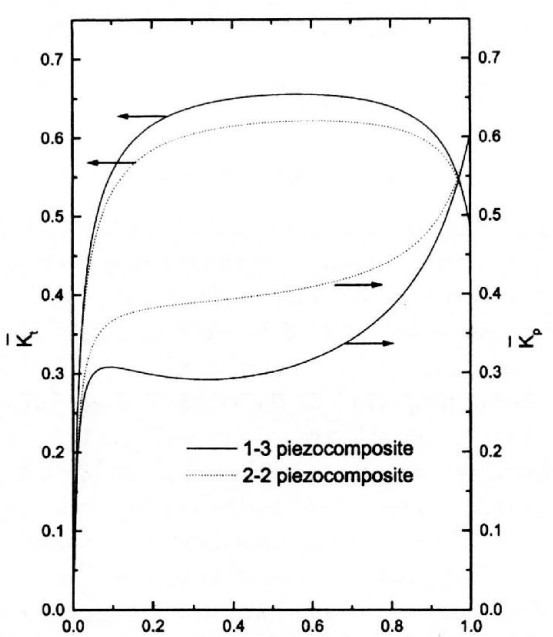

FIG. 2. Plot of electromechanical coupling coefficients $\overline{K}_t$ and $\overline{K}_p$ versus volume fraction of piezoelectric. The laminate composite 2–2 (continuous line) and the fibrous composite 1–3 (dotted line).

The analytical expressions that were derived using the "double homogenization" method can equally be used for a passive or piezoelectric matrix. The second example is for a 1–3 composite of $TLZ-5$ piezoelectric rods embedded in a piezoelectric copolymer $VDR/TrFE$. The properties are displayed in Table 1. In Fig. 3(a–f), the parameters: short-circuit stiffness constant (E-constant) $\overline{C}_{33}$, open-circuit stiffness constant (D-constant) $\overline{C}_{33}^{D}$ and dielectric constant $\overline{\varepsilon}_{33}^{T}/\varepsilon_0$, specific acoustic impedance $\overline{Z}$, electromechanical coupling constant $\overline{K}_t$, longitudinal wave speed $\overline{V}_l$ are plotted against volume fraction of the fibers, respectively. The continuous curve is the result of computation using the model proposed by the authors. The dotted curve for the *approximate theory* and the bullet points of the experimental results were reported in [11]. The agreement is seen to be quite good. The theoretical values show essentially the same trend as the experimental data [11] as well as the *approximate theory* used in [11] which was introduced by Smith and Auld (see, [4–5]). In this sense, six simplifying approximations to extract the essential physics are introduced en [4] and [5]. In connection with that, the main assumptions can be summarized as follows. First, the authors assume that the strain and electric field are independent of x and y throughout the individual phases. This is clearly not true in detail, as finite element calculations reveal. The expectation is that this approximation captures the physical behavior in an average sense. Second, they add the usual simplifications made in analyzing the thickness mode oscillations in a large, thin, electrode plate (symmetry in the $x-y$ plane, $E_1 = E_2 = 0$, etc). The third approximation embodies the picture that the ceramic and polymer move together in a uniform thickness oscillation. Thus the vertical strains (in the z direction) are the same in both phases. This is clearly not always true as the laser probe measurements of the displacements of oscillating composite plates reveal. Fourth, they describe the electric fields in two phases. Since the faces of the composite plates are equi-potential, they take the electrofields to be the same in both phases. Fifth approximation concerns the lateral interaction between the phases. They assume that the lateral stresses are equal in both phases and that the lateral strain in ceramics is compensated by a complementary strain in the polymer, so that the composite as a whole is laterally clamped. Sixth approximation deals with the dependent coordinates. Since the lateral periodicity is sufficiently fine, the authors obtain the effective total stress and electric displacement by averaging over the contributions of the constituent phases (rule of phases for both x_3-components of strains and electric displacement).

Note that the results of the "simple" physical analysis of Auld–Smith [4–5] agree remarkably well with the "rational" homogenization method, while the Auld–Smith results concern a thin plate with square inclusions whereas the "double homogenization" technique is applied to a body which is infinite in di-

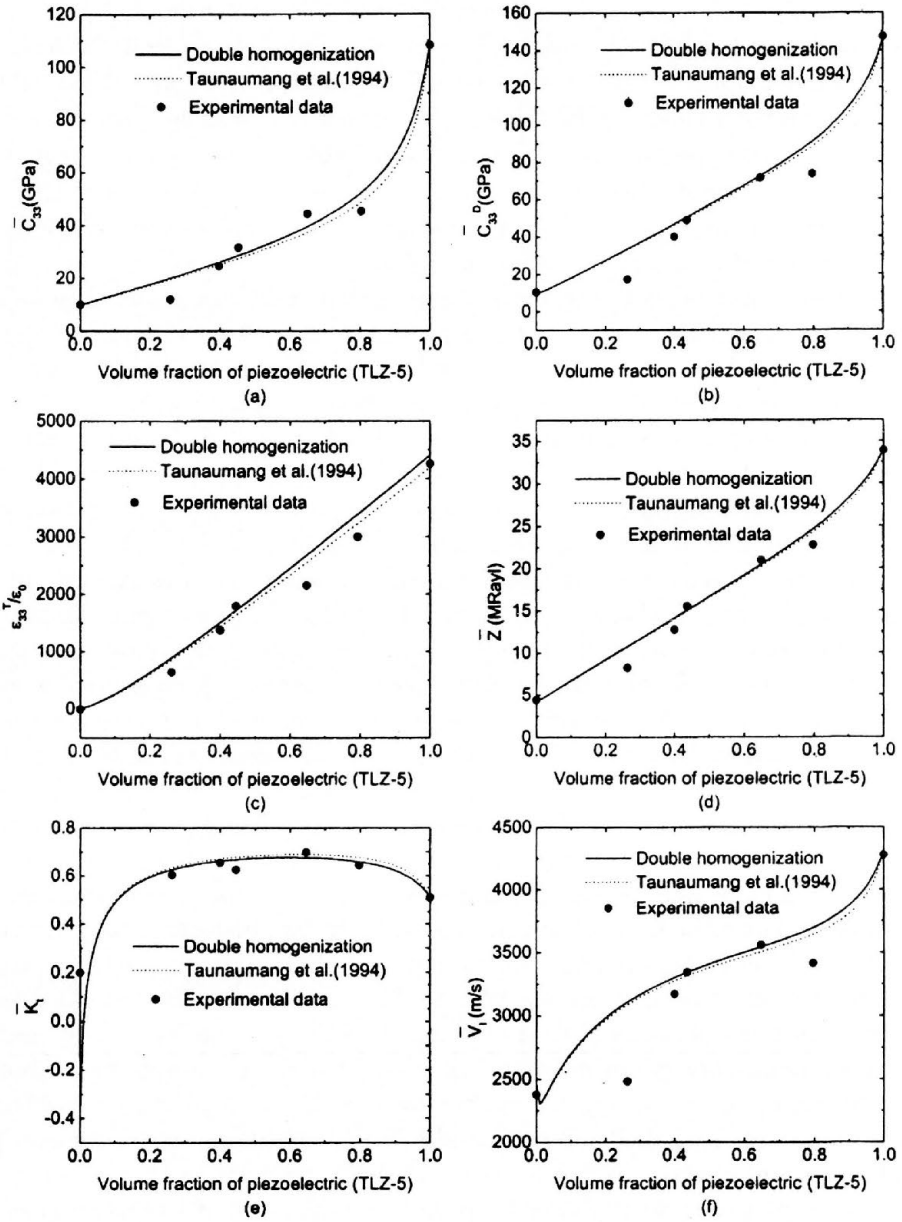

FIG. 3. Comparison between the "double asymptotic homogenization" with the theoretical and experimental results: (a) short-circuit stiffness constant (E-constant) $\overline{C}_{33}$, (b) open-circuit stiffness constant (D-constant) $\overline{C}_{33}^{D}$, (c) dielectric constant $\overline{\varepsilon}_{33}^{T}/\varepsilon_0$, (d) acoustic impedance $\overline{Z}$, (e) electromechanical coupling constant $\overline{K}_t$, (f) stiffened longitudinal velocity $\overline{V}_l$.

rection x_3. This may correspond to different hypotheses concerning the states of stress and strains in the body as in the case in a plate and the cross-section of an infinite cylinder. This may explain the difference observed the last value $\overline{d}_h$. This hydrostatic charge coefficient $\overline{d}_h$ is plotted as a function of the fiber volume fraction in Fig. 4. The solid line for the values are obtained using the"double asymptotic homogenization" method. The dotted line for the calculated values and the experimental bullet points were taken from [11]. This proves that the agreement between the experimental data and the "double homogenization" prediction is very good.

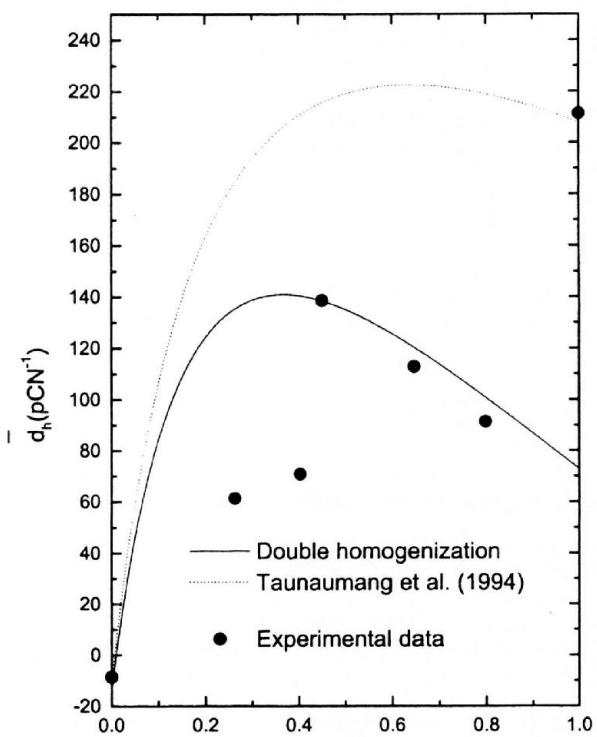

FIG. 4. The hydrostatic charge constant $\overline{d}_h$ versus fiber volume fraction.

Acknowledgments

This work was supported by the Cuban Nuclear Energy and Advanced Technology Agency and the projects PAPIIT, DGAPA, UNAM IN103301. Thanks are due to Miss Ana Pérez Areteaga for her computational support. The authors would like to thank Prof. Martin Ostoja–Starzewski (McGill University) for some

useful comments. The work was completed while the author RRR was visiting the Laboratoire de Modélisation en Mécanique from Université Pierre et Marie Curie, Paris. G.A.M benefits from a Max-Planck Award for International Cooperation (2002–2005).

References

1. A. A. GREKOV, S. O. KRAMAROV and A. A. KUPRIENKO, *Effective properties of a transversely isotropic piezocomposite with cylindrical inclusions*, Ferroelectrics, **76**, 43–48, 1987.

2. Y. BENVENISTE and G. J. DVORAK, *Uniform fields and universal relations in piezoelectric composites*, J. Mech. Phys. Solids **40**, 1295–1312, 1992.

3. F. CRACIUN, L. SORBA, E. MOLINARI and M.PAPPALARDO, *A coupled-mode theory for periodic piezoelectric composites*, IEEE Trans. Ultrason. Ferroelectr. and Freq. Control, **36**, 50–56, 1989.

4. W. A. SMITH and B. A. AULD, *Modeling 1–3 composite piezoelectrics: thickness-mode oscillations*, IEEE Trans. Ultrason. Ferroelectr. and Freq. Control, **38**, 40–47, 1991.

5. W. A. SMITH, *Modeling 1–3 composite piezoelectrics: hydrostatic response*, IEEE Trans. Ultrason. Ferroelectr. and Freq. Control, **40**, 41–49, 1993.

6. A. GALKA, J. J. TELEGA and R. WOJNAR, *Some computational aspects of homogenization of thermopiezoelectric composites*, Comput. Assisted Mech. Engng. Sci. **3**, 133–154, 1996.

7. J. B. CASTILLERO, J. A. OTERO, R. R. RAMOS and A. BOURGEAT, *Asymptotic homogenization of laminated piezocomposite materials*, Int. J. Solids Struct., **35**, 527–541, 1998.

8. J. PASTOR, *Homogenization of linear piezoelectric media*, Mech. Res. Commun., **24**, 145–150, 1997.

9. IGOR V. ANDRIANOV, V. V. DANISHEVSKIĬ and DIETER WEICHERT, *Asymptotic determination of effective elastic properties of composite materials with fibrous square-shaped inclusions*, Eur. J. Mech. A/Solids, **21**, 1019–1036, 2002.

10. I. V. ANDRIANOV, G. A. STARUSHENKO, V. V. DANISHEVSKIĬ and S. TOKARZEWSKI, *Homogenization procedure and Padé approximants for effective heat conductivity of composite materials with cylindrical inclusions having square cross section*, Proc. R. Soc. Lond. A, **455**, 3401–3413, 1999.

11. H. TAUNAUMANG, I. L. GUY and H. L. W. CHAN, *Electromechanical properties of 1–3 piezoelectric ceramic/piezoelectric polymer composites*, J. Appl. Phys. **76**, 484–489, 1994.

12. K. SCHULGASSER, *Relationships between the effective properties of transversely isotropic piezoelectric composites*, J. Mech. Phys. Solids **40**, 473–479, 1992.

13. R. GUINOVART-DÍAZ, J. BRAVO-CASTILLERO, R. RODRÍGUEZ-RAMOS and F. J. SABINA, *Closed-form expressions for the effective coefficients of fibre-reinforced composite with transversely isotropic constituents. I. Elastic and hexagonal symmetry*, J. Mech. Phys. Solids, **49**, 1445–1462, 2001.

14. F. J. SABINA, R. RODRÍGUEZ-RAMOS, J. BRAVO-CASTILLERO and R. GUINOVART-DÍAZ, *Closed-form expressions for the effective coefficients of fibre-reinforced composite with transversely isotropic constituents. I. Piezoelectric and hexagonal symmetry*, J. Mech. Phys. Solids, **49**, 1463–1479, 2001.

15. R. RODRÍGUEZ-RAMOS, F. J. SABINA, R. GUINOVART-DÍAZ and J. BRAVO-CASTILLERO, *Closed-form expressions for the effective coefficients of a fiber-reinforced composite with transversely isotropic constituents. I. Elastic and square symmetry*, Mech. Mat., **33**, 223–235, 2001.

16. J. BRAVO-CASTILLERO, R. GUINOVART-DÍAZ, F. J. SABINA and R. RODRÍGUEZ-RAMOS, *Closed-form expressions for the effective coefficients of a fiber-reinforced composite with transversely isotropic constituents. II. Piezoelectric and square symmetry*, Mech. Mat., **33**, 237–248, 2001.

17. R. GUINOVART-DÍAZ, J. BRAVO-CASTILLERO, R. RODRÍGUEZ-RAMOS and F. J. SABINA, *Overall properties of piezocomposite materials 1–3*, Mat. Lett., **48**, 93–98, 2001.

18. D. A. BERLINCOURT, D. R. CURRAN and H. JAFFE, *Piezoelectric and piezomagnetic materials and their function in transducers*, Phys. of Acoust., **1A**, W. P. MASON [Ed.] Academic Press, New York 1964.

Received February 28, 2002.

Arch. Mech., **55**, 4, pp. 373–387, Warszawa 2003

Some more inverse solutions for steady flows of a second-grade fluid

A. M. SIDDIQUI[(1)], M. R. MOHYUDDIN[(2)], T. HAYAT[(2)], S. ASGHAR[(3)]

[(1)] *Pennsylvania State University, York Campus, York, PA* 17403, *USA*

[(2)] *Department of Mathematics, Quaid-i-Azam University, Islamabad 45320, Pakistan*

[(3)] *COMSATS, Institute of Information Technology, Abbottabad, Pakistan*

INVERSE SOLUTIONS of the equations of motion of an incompressible second-grade fluid are obtained by assuming certain forms of the stream function. Expressions for streamlines, velocity components and pressure distributions are given in each case and are compared with the known results.

Key words: second-grade fluid; exact solutions; two moving parallel disks.

Notations

$\mathbf{T}$	Cauchy stress tensor,
$-p\mathbf{I}$	indeterminate spherical stress,
μ	viscosity,
α_1	elasticity,
α_2	cross-viscosity,
$\mathbf{A}_1, \mathbf{A}_2$	Rivlin–Ericksen tensors,
$\mathbf{V}$	velocity,
grad	the gradient operator,
d/dt	material time derivative,
$\top$	the transpose,
ρ	density,
χ	the body force,
∇^2	the Laplacian operator,
$\mathbf{V}_t$	$\partial \mathbf{V}/\partial t$,
$\lvert\mathbf{A}_1\rvert$	the usual norm of matrix $\mathbf{A}_1$,
u, v, w	the velocity components,
x, y, z	the coordinate axis,
ϕ	relative velocity of the disk,
$\widehat{p}$	modified pressure,
$\{\cdot, \cdot\}$	Poisson bracket,
ω	vorticity vector,

ν kinematic viscosity,
Λ second-grade parameter,
ψ the stream function.

1. Introduction

RHEOLOGICAL PROPERTIES of materials are specified in general by their so called constitutive equations. The simplest constitutive equation for a fluid is a Newtonian one and the classical Navier–Stokes theory is based on this equation. The mechanical behaviour of many real fluids, especially those of low molecular weight, is well enough described by this theory. However, in many fields, such as food industry, drilling operations and bio-engineering, the fluids, either synthetic or natural, are mixtures of different stuffs such as water, particle, oils, red cells and other long chain molecules; this combination imparts strong non-Newtonian characteristics to the resulting liquids; the viscosity function varies non-linearly with the shear rate; elasticity is felt through elongational effects and time-dependent effects. In these cases, the fluids have been treated as viscoelastic fluids. Because of the difficulty to suggest a single model which exhibits all properties of viscoelastic fluids, they cannot be described simply as Newtonian fluids. For this reason, many models or constitutive equations have been proposed and most of them are empirical or semi-empirical. One of the simplest types of models to account for the rheological effects of viscoelastic fluid is the second-grade model. Further, the equations governing the flow of a second-grade fluids are one order higher than the Navier–Stokes equations. A marked difference between the case of the Navier–Stokes theory and that for fluids of second-grade is that, ignoring the non-linearity in the Navier–Stokes equation does not lower the order of the equation; however, ignoring the higher order non-linearities in the case of second-grade fluid reduces the order of the equation. The no-slip boundary condition is insufficient for a second-grade fluid and therefore, one needs an additional boundary condition. A critical review on the boundary condition, the existence and uniqueness of the solution has been given by RAJAGOPAL [1].

The governing equations that describe the flow of a Newtonian fluid is the Navier–Stokes equations. These equations are nonlinear partial differential equations and known exact solutions are few in number. Exact solutions are very important not only because they are solutions of some fundamental flows but also because they serve as accuracy checks for experimental, numerical and asymptotic methods. Since the equations of motion of non-Newtonian fluids are more complicated and nonlinear than the Navier–Stokes equations, so the inverse methods described by NEMENYI [2] have become attractive. In these methods, solutions are found by assuming certain physical or geometrical properties of the flow field. KALONI and HUSCHILT [3], SIDDIQUI and KALONI [4], SIDDIQUI [5],

BENHARBIT and SIDDIQUI [6] and LABROPULU [7] used this method to study the flow problems of a second-grade fluid.

In this paper we discuss the second-grade fluid motion between two parallel disks/plates, moving towards each other or in opposite directions with a constant disk velocity. For such a fluid equations are modeled for a grade of fluid two and are solved by assuming certain form of the stream function. The graphs are plotted explicitly in the functional form to see the behaviour of the flow field.

The paper is organized as follows. In Sec. 2, basic equations and formulation of the problem is given. Section 3 consists of some special flows called the Riabounchinsky type flows and finally, in Sec. 4, concluding remarks are given. Stream function, velocity components and the pressure fields are derived in each case. Moreover, the streamlines are plotted in each case to see the flow behaviour.

2. Governing equations

The constitutive equation of an incompressible fluid of second-grade is of the form [8]

$$\mathbf{T} = -p\mathbf{I} + \mu\mathbf{A}_1 + \alpha_1\mathbf{A}_2 + \alpha_2\mathbf{A}_1^2, \tag{2.1}$$

where $\mathbf{T}$ is the Cauchy stress tensor, $-p\mathbf{I}$ denotes the indeterminate spherical stress and μ, α_1 and α_2 are measurable material constants. They denote, respectively, the viscosity, elasticity and cross-viscosity. These material constants can be determined from viscometric flows for any real fluid. $\mathbf{A}_1$ and $\mathbf{A}_2$ are Rivlin–Ericksen tensors [8] and they denote, respectively, the rate of strain and acceleration. $\mathbf{A}_1$ and $\mathbf{A}_2$ are defined by

$$\mathbf{A}_1 = (\mathrm{grad}\mathbf{V}) + (\mathrm{grad}\mathbf{V})^{\top}, \tag{2.2}$$

$$\mathbf{A}_2 = \frac{d\mathbf{A}_1}{dt} + \mathbf{A}_1(\mathrm{grad}\mathbf{V}) + (\mathrm{grad}\mathbf{V})^{\top}\mathbf{A}_1. \tag{2.3}$$

Here $\mathbf{V}$ is the velocity, grad the gradient operator, $\top$ the transpose, and d/dt the material time derivative.

The basic equations governing the motion of an incompressible fluid are

$$\mathrm{div}\mathbf{V} = 0, \tag{2.4}$$

$$\rho\frac{d\mathbf{V}}{dt} = \rho\boldsymbol{\chi} + \mathrm{div}\mathbf{T}, \tag{2.5}$$

where ρ is the density and $\boldsymbol{\chi}$ the body force.

Inserting (2.1) in (2.5) and making use of (2.2) and (2.3) we obtain the following vector equation

$$\text{grad}\left[\frac{1}{2}\rho|\mathbf{V}|^2 + p - \alpha_1\left(\mathbf{V}\cdot\nabla^2\mathbf{V} + \frac{1}{4}|\mathbf{A}_1|^2\right)\right] + \rho[\mathbf{V}_t - \mathbf{V}\times(\nabla\times\mathbf{V})] \tag{2.6}$$

$$= \mu\nabla^2\mathbf{V} + \alpha_1\left[\nabla^2\mathbf{V}_t + \nabla^2(\nabla\times\mathbf{V})\times\mathbf{V}\right] + (\alpha_1+\alpha_2)\,\text{div}\mathbf{A}_1^2 + \rho\chi,$$

in which ∇^2 is the Laplacian operator, $\mathbf{V}_t = \partial\mathbf{V}/\partial t$, and $|\mathbf{A}_1|$ is the usual norm of matrix $\mathbf{A}_1$. If this model is required to be compatible with thermodynamics, then the material constants must meet the restrictions [9, 10]

$$\mu \geq 0, \qquad \alpha_1 \geq 0, \qquad \alpha_1 + \alpha_2 = 0. \tag{2.7}$$

On the other hand, experimental results of the tested fluids of second-grade showed that $\alpha_1 < 0$ and $\alpha_1 + \alpha_2 \neq 0$ which contradicts the above conditions and implies that such fluids are unstable. This controversy is discussed in detail in [1]. However, in this paper we will discuss both cases, $\alpha_1 \geq 0$ and $\alpha_1 < 0$.

We consider two parallel disks/plates in water and start moving them towards each other or in opposite directions (considering the size of the disks much larger than the distance between them). One can observe that when the disks are approaching each other, the effort required is smaller than that when the disks are moving apart. It can be discussed and explained by considering the different nature of the fluid motion. When the disks are approaching each other it is of potential type and when they are moving away then that is of rotational nature.

For such consideration, various authors [11, 13, 14] assumed that the horizontal components of the velocity u, v, do not depend on the vertical coordinate, z, whereas the vertical velocity w depends linearly on the distance between the disks. Thus the velocity field is of the following form [15]:

$$\mathbf{V}(x,y,z,t) = [u(x,y,t),\ v(x,y,t),\ -2\phi z], \tag{2.8}$$

where ϕ is the relative velocity of the disk, considered here to be constant.

Inserting (2.8) in (2.4) and (2.6) and making use of the assumption (2.7) we obtain, in the absence of body forces, the following equations:

$$\frac{\partial u}{\partial x} + \frac{\partial v}{\partial y} = 2\phi, \tag{2.9}$$

$$\frac{\partial\widehat{p}}{\partial x} + \rho\left[\frac{\partial u}{\partial t} - v\omega\right] = \left(\mu + \alpha_1\frac{\partial}{\partial t}\right)\nabla^2 u - \alpha_1 v\nabla^2\omega, \tag{2.10}$$

$$\frac{\partial\widehat{p}}{\partial y} + \rho\left[\frac{\partial v}{\partial t} + u\omega\right] = \left(\mu + \alpha_1\frac{\partial}{\partial t}\right)\nabla^2 v + \alpha_1 u\nabla^2\omega, \tag{2.11}$$

where

$$\omega = \frac{\partial v}{\partial x} - \frac{\partial u}{\partial y}, \tag{2.12a}$$

$$\widehat{p} = p + \frac{1}{2}\rho\left(u^2 + v^2 + 4\phi^2 z^2\right) - \alpha_1\left[u\nabla^2 u + v\nabla^2 v + \frac{1}{4}\left|\mathbf{A}_1^2\right|\right], \tag{2.12b}$$

$$\left|\mathbf{A}_1^2\right| = 4\left(\frac{\partial u}{\partial x}\right)^2 + 4\left(\frac{\partial v}{\partial y}\right)^2 + 16\phi^2 + 2\left(\frac{\partial u}{\partial y} + \frac{\partial v}{\partial x}\right)^2. \tag{2.12c}$$

REMARK 1. On setting $\alpha_1 = 0$ in (2.10) and (2.11) we recover the equations for Newtonian fluid [11].

Equations (2.9)–(2.11) are three partial differential equations for three unknown functions u, v and $\widehat{p}$ of the variables (x, y). Once the velocity field is determined, the pressure field (2.12b) can be calculated by integrating (2.10) and (2.11). Note that the equation for the vertical component w is identically zero.

Eliminating pressure in (2.10) and (2.11), by applying the integrability condition $\partial^2\widehat{p}/\partial x\partial y = \partial^2\widehat{p}/\partial y\partial x$, we get the compatibility equation

$$\rho\left[\frac{\partial\omega}{\partial t} + 2\phi\omega + \left(u\frac{\partial}{\partial x} + v\frac{\partial}{\partial y}\right)\omega\right] = \left(\mu + \alpha_1\frac{\partial}{\partial t}\right)\nabla^2\omega + \alpha_1\left[\left(u\frac{\partial}{\partial x} + v\frac{\partial}{\partial y}\right)\nabla^2\omega + 2\phi\nabla^2\omega\right]. \tag{2.13}$$

Let us consider the potential component from the horizontal components of the velocity and introduce the flow function of the following form:

$$u = \phi x + \frac{\partial\psi}{\partial y}, \qquad v = \phi y - \frac{\partial\psi}{\partial x}, \tag{2.14}$$

where $\psi(x, y)$ is the stream function. We see that the continuity equation (2.9) is satisfied identically and (2.14) in (2.13) yields the following equation:

$$\rho\left[\left(2\phi + \frac{\partial}{\partial t}\right)\nabla^2\psi + \phi\left(x\frac{\partial}{\partial x} + y\frac{\partial}{\partial y}\right)\nabla^2\psi - \{\psi, \nabla^2\psi\}\right] = \left(\mu + \alpha_1\frac{\partial}{\partial t}\right)\nabla^4\psi + \alpha_1\left[2\phi\nabla^4\psi + \phi\left(x\frac{\partial}{\partial x} + y\frac{\partial}{\partial y}\right)\nabla^4\psi - \{\psi, \nabla^4\psi\}\right], \tag{2.15}$$

in which

$$\nabla^4 = \nabla^2 \cdot \nabla^2, \qquad \omega = -\nabla^2\psi$$

and

$$\{\psi, \nabla^2\psi\} = \frac{\partial\psi}{\partial x}\frac{\partial\left(\nabla^2\psi\right)}{\partial y} - \frac{\partial\psi}{\partial y}\frac{\partial\left(\nabla^2\psi\right)}{\partial x}$$

is the Poisson bracket.

REMARK 2. The solution $\psi = 0$ of (2.15), corresponds to liquid potential motion, known as the motion near the stagnation point.

3. Solutions of some special types

We consider *Riabounchinsky type flows* in order to solve (2.15).

3.1. Solution of the type $\psi(x, y) = y\xi(x)$

In order to obtain a class of solution of (2.15) we substitute

$$\psi(x, y) = y\xi(x) \tag{3.1}$$

into (2.15) and get the following equation

$$\rho\left[\phi\left(3\xi'' + x\xi'''\right) - \left(\xi'\xi'' - \xi\xi'''\right)\right] = \mu\xi^{IV} + \alpha_1\begin{bmatrix} \phi\left(3\xi^{IV} + x\xi^{V}\right) \\ -\left(\xi'\xi^{IV} - \xi\xi^{V}\right) \end{bmatrix}, \tag{3.2}$$

where $\xi(x)$ is an arbitrary function of x and primes denote the derivative with respect to x.

Integrating (3.2) once and equating the constant of integration equal to zero we obtain

$$\mu\xi''' + \rho\left[\left(\xi'^2 - \xi\xi''\right) - \phi\left(2\xi' + x\xi''\right)\right] - \alpha_1\begin{bmatrix} \left(-\xi\xi^{IV} + 2\xi'\xi''' - \xi''^2\right) \\ -\phi\left(2\xi''' + x\xi^{IV}\right) \end{bmatrix} = 0. \tag{3.3}$$

For the solution of the equation (3.2) we write

$$\xi(x) = \delta\left(1 + \lambda e^{\sigma x}\right) - \phi x \tag{3.4}$$

in which δ, σ and λ are arbitrary real constants. Making use of (3.4) into (3.2) we have

$$\delta = \frac{\mu\sigma}{\rho - \alpha_1\sigma^2} - \frac{4\phi}{\sigma} \tag{3.5}$$

and thus from (3.1)

$$\psi(x,y) = \left[\frac{\mu\sigma}{\rho - \alpha_1\sigma^2} - \frac{4\phi}{\sigma}\right] y\,(1 + \lambda e^{\sigma x}) - \phi x y. \tag{3.6}$$

The velocity components (2.14) and the pressure field (2.12*b*) become

$$u = \left[\frac{\mu\sigma}{\rho - \alpha_1\sigma^2} - \frac{4\phi}{\sigma}\right](1 + \lambda e^{\sigma x}), \tag{3.7}$$

$$v = 2\phi y - \left[\frac{\mu\sigma}{\rho - \alpha_1\sigma^2} - \frac{4\phi}{\sigma}\right] y\lambda\sigma e^{\sigma x}. \tag{3.8}$$

$$p = p_0 + \mu\bar{a}\lambda\sigma\left(1 - \frac{\sigma^2 y^2}{2}\right)e^{\sigma x} - \frac{1}{2}\rho\left[\bar{a}^2 + 4\phi^2\left(y^2 + z^2\right) - \bar{a}^2\lambda^2 e^{2\sigma x}\right] \tag{3.9}$$

$$+ \alpha_1\left[\bar{a}\lambda\sigma\left(\bar{a}\sigma - 2\phi\sigma^2 y^2 - 4\phi\right)e^{\sigma x} + \bar{a}^2\lambda^2\sigma^2\left(3 + \frac{\sigma^2 y^2}{2}\right)e^{2\sigma x} + 8\phi^2\right],$$

where p_0 is an arbitrary constant, known as the reference pressure.

The streamline flow for $\psi = \Omega_1$ is given by the functional form

$$y = \frac{\Omega_1}{(1 + \lambda e^{\sigma x})\,\varepsilon - x\phi}, \tag{3.10}$$

where

$$\varepsilon = \frac{\nu\sigma}{1 - \Lambda\sigma^2} - \frac{4\phi}{\sigma}$$

in which ν is the kinematic viscosity and Λ is the second-grade parameter.

Figure 1 shows the streamlines for $\phi = \sigma = \lambda = 1$, $\mu/\rho = 0.5$, $\alpha_1/\rho = 0.1$, $\psi = 15, 20, 25, 30, 40$.

3.2. Solutions of the type $\psi(x,y) = y\xi(x) + \eta(x)$

Inserting

$$\psi(x,y) = y\xi(x) + \eta(x) \tag{3.11}$$

in (2.15) we obtain the following equation

$$\rho\left[\begin{array}{r} 2\phi\,(y\xi'' + \eta'') + \phi\{y\,(\xi'' + x\xi''') + x\eta'''\} \\ -\{y\,(\xi'\xi'' - \xi\xi''') + (\eta'\xi'' - \xi\eta''')\} \end{array}\right] = \mu\left(y\xi^{IV} + \eta^{IV}\right) \tag{3.12}$$

$$+ \alpha_1\left[\begin{array}{r} 2\phi\left(y\xi^{IV} + \eta^{IV}\right) + \phi\{y\left(\xi^{IV} + x\xi^{V}\right) + x\eta^{V}\} \\ -\{y\left(\xi'\xi^{IV} - \xi\xi^{V}\right) + \left(\eta'\xi^{IV} - \xi\eta^{V}\right)\} \end{array}\right].$$

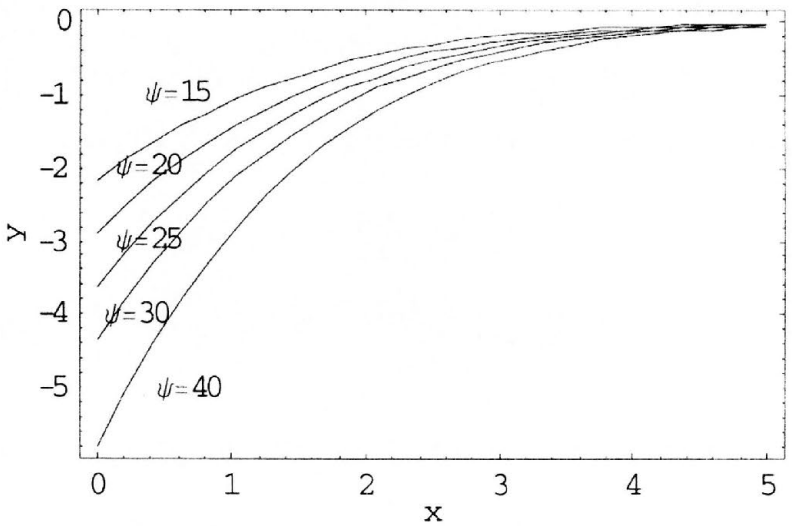

FIG. 1. Streamline flow pattern for $\psi(x,y) = \left[\frac{\mu\sigma}{\rho - \alpha_1\sigma^2}\frac{-4\phi}{\sigma}\right] y\left(1 + \lambda e^{\sigma x}\right) - \phi xy$.

From above equation we have

$$\rho\left[\left(\xi'\xi'' - \xi\xi'''\right) - \phi\left(3\xi'' + x\xi'''\right)\right] + \mu\xi^{IV} - \alpha_1\begin{bmatrix}\left(\xi'\xi^{IV} - \xi\xi^{V}\right)\\ -\phi\left(3\xi^{IV} + x\xi^{V}\right)\end{bmatrix} = 0, \tag{3.13}$$

and

$$\rho\left[\left(\eta'\xi'' - \xi\eta'''\right) - \phi\left(2\eta'' + x\eta'''\right)\right] + \mu\eta^{IV} - \alpha_1\begin{bmatrix}\left(\eta'\xi^{IV} - \xi\eta^{V}\right)\\ -\phi\left(3\eta^{IV} + x\eta^{V}\right)\end{bmatrix} = 0, \tag{3.14}$$

where $\xi(x)$ and $\eta(x)$ are arbitrary functions of its arguments. Integrating (3.13) and (3.14) and then taking the constants of integration equal to zero we have

$$\mu\xi''' + \rho\left[\left(\xi'^2 - \xi\xi''\right) - \phi\left(2\xi' + x\xi''\right)\right] - \alpha_1\begin{bmatrix}\left(-\xi\xi^{IV} + 2\xi'\xi''' - \xi''^2\right)\\ -\phi\left(2\xi''' + x\xi^{IV}\right)\end{bmatrix} = 0, \tag{3.15}$$

$$\mu\eta''' + \rho\left[\left(\eta'\xi' - \xi\eta''\right) - \phi\left(2\eta' + x\eta''\right)\right] - \alpha_1\begin{bmatrix}\xi'\eta''' - \xi\eta^{IV} + \eta'\xi'''\\ -\eta''\xi'' - \phi\left(2\eta''' + x\eta^{IV}\right)\end{bmatrix} = 0. \tag{3.16}$$

We note that (3.13) is similar to (3.2). Its solution is given in (3.4). Substituting (3.4) into (3.13) we have

$$\alpha_1\overline{a}\,(1+\lambda e^{\sigma x})\,\eta^{V}+(\mu+3\alpha_1\phi)\,\eta^{IV}-\rho\overline{a}\,(1+\lambda e^{\sigma x})\,\eta'''-2\rho\phi\eta''+\overline{a}\lambda\sigma^2\left(\rho-\alpha_1\sigma^2\right)e^{\sigma x}\eta'=0, \tag{3.17}$$

where

$$\overline{a}=\frac{\mu\sigma}{\rho-\alpha_1\sigma^2}-4\frac{\phi}{\sigma}.$$

We note that it is not easy to obtain the general solution of (3.17). In order to find its solution we consider the following special cases:

CASE 1. When $\alpha_1\neq 0,\quad \phi\neq 0,\quad \sigma=1,\quad \lambda=0$

then (3.17) reduces to

$$\alpha_1\overline{a}\eta^{V}+(\mu+3\alpha_1\phi)\,\eta^{IV}-\rho\overline{a}\eta'''-2\rho\phi\eta''=0. \tag{3.18}$$

We see that (3.18) is of fifth order and in order to solve it we reduce its order by putting $\eta''=\overline{A}\,(x)$ such that (3.18) becomes

$$\alpha_1\overline{a}\overline{A}'''+(\mu+3\alpha_1\phi)\,\overline{A}''-\rho\overline{a}\overline{A}'-2\rho\phi\overline{A}=0. \tag{3.19}$$

On substituting $\overline{A}(x)=\widehat{P}(x)e^{x}$, (3.19) takes the form

$$\alpha_1\overline{a}\left(3\widehat{P}'+3\widehat{P}''+\widehat{P}'''\right)e^{x}+(\mu+3\alpha_1\phi)\left(2\widehat{P}'+\widehat{P}''\right)e^{x}-\rho\overline{a}\widehat{P}'e^{x}=0. \tag{3.20}$$

Finally, $\widehat{P}'\,(x)=R\,(x)$ converts (3.20) into a second order differential equation

$$\alpha_1\overline{a}R''+(\mu+3\alpha_1\,(\phi+\overline{a}))\,R'-[(3\alpha_1-\rho)\,\overline{a}+2\mu+6\alpha_1\phi]\,R=0. \tag{3.21}$$

The solution of above equation is

$$R\,(x)=A_3\exp\left(\frac{-c-\sqrt{c^2-4d}}{2}\right)x+A_4\exp\left(\frac{-c+\sqrt{c^2-4d}}{2}\right)x, \tag{3.22}$$

where A_3 and A_4 are arbitrary constants and

$$c=\frac{3\alpha_1\,(\overline{a}+\phi)+\mu}{\alpha_1\overline{a}},$$

$$d=\frac{3\alpha_1\,(\overline{a}+2\phi)+2\mu-\rho\overline{a}}{\alpha_1\overline{a}},$$

$$\overline{a}=\frac{\mu}{\rho-\alpha_1}-4\phi.$$

In order to find $\eta(x)$ we make backward substitutions and finally obtain the form

$$\eta(x) = \frac{A_3}{m_1(1+m_1)^2}e^{(1+m_1)x} + \frac{A_4}{m_2(1+m_2)^2}e^{(1+m_2)x} + A_5e^x + A_6x + A_7, \tag{3.23}$$

where A_i $(i = 5, 6, 7)$ are constants of integration and

$$m_1 = \frac{-c - \sqrt{c^2 - 4d}}{2}, \qquad m_2 = \frac{-c + \sqrt{c^2 - 4d}}{2}.$$

From (3.4), (3.11) and (3.13) we get

$$\psi(x,y) = y\left[\frac{\mu}{\rho - \alpha_1} - \phi(4+x)\right] + A_5e^x + A_6x + A_7 + \frac{A_3}{m_1(1+m_1)^2}e^{(1+m_1)x} + \frac{A_4}{m_2(1+m_2)^2}e^{(1+m_2)x}. \tag{3.24}$$

The velocity components and pressure field are

$$u = \frac{\mu}{\rho - \alpha_1} - 4\phi, \tag{3.25}$$

$$v = 2\phi y - \left[\frac{A_3}{m_1(1+m_1)}e^{(1+m_1)x} + \frac{A_4}{m_2(1+m_2)}e^{(1+m_2)x} + A_5e^x + A_6\right], \tag{3.26}$$

$$p = p_0 - \frac{1}{2}\rho\left[a_1^2 + A_6^2 + 4\phi^2(y^2+z^2) - 4y\phi A_6\right] + \alpha_1\left[\frac{A_3^2}{m_1^2}e^{2(1+m_1)x} + \frac{2A_3A_4}{m_1m_2}e^{(2+m_1+m_2)x} + \frac{A_4^2}{m_2^2}e^{2(1+m_2)x} + A_5^2e^{2x}4\phi^2 + \frac{2A_3A_5(2+3m_1+m_1^2)}{(2+m_1)m_1(1+m_1)}e^{(2+m_1)x} + \frac{2A_4A_5(2+3m_2+m_2^2)}{(2+m_2)m_2(1+m_2)}e^{(2+m_2)x}\right]. \tag{3.27}$$

The streamline for $\psi = \Omega_2$ is given by the functional form

$$(3.28) \qquad y = -\frac{1}{\varepsilon_1 - x\phi} \times \left[-\Omega_2 + \frac{A_3}{m_1 (1+m_1)^2} e^{(1+m_1)x} + \frac{A_4}{m_2 (1+m_2)^2} e^{(1+m_2)x} + A_5 e^x + A_6 x + A_7 \right],$$

where

$$\varepsilon_1 = \frac{\nu}{1-\Lambda} - 4\phi, \qquad a_1 = \frac{\mu}{\rho - \alpha_1} - 4\phi.$$

Streamline pattern is plotted in Fig. 2 for $\phi = a = \lambda = 1$, $\mu/\rho = 0.5$, $\alpha_1/\rho = 0.1$, $A_3 = A_4 = A_5 = A_6 = A_7 = 1$, $\psi = 15, 20, 25, 30, 40$.

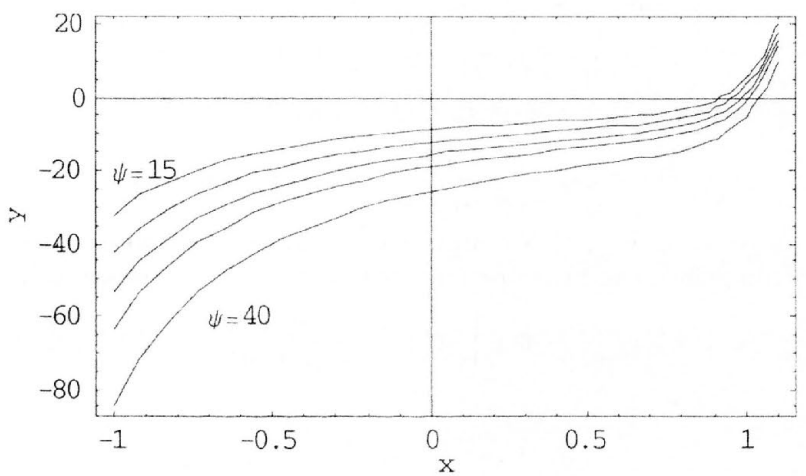

FIG. 2. Streamline flow pattern for $\psi(x,y) = y\left[\frac{\mu}{\rho-\alpha_1} - \phi(4+x)\right] + A_5 e^x + A_6 x + A_7 + \frac{A_3}{m_1(1+m_1)^2} e^{(1+m_1)x} + \frac{A_4}{m_2(1+m_2)^2} e^{(1+m_2)x}$.

CASE 2. When $\alpha_1 \neq 0, \quad \phi = 0, \quad \sigma = 1, \quad \lambda \neq 0$

then (3.17) reduces to

$$(3.29) \qquad \alpha_1 (1+\lambda e^x)\eta^V + (\rho - \alpha_1)\eta^{IV} - \rho(1+\lambda e^x)\eta''' + (\rho - \alpha_1)\lambda e^x \eta' = 0.$$

To obtain the solution of (3.29) we try to reduce its order. For this purpose we put $\eta' = \widehat{A}(x)$ which leaves (3.29) into a form which is one order less, that is

$$(3.30) \qquad \alpha_1 (1+\lambda e^x)\widehat{A}^{IV} + (\rho - \alpha_1)\widehat{A}''' - \rho(1+\lambda e^x)\widehat{A}'' + (\rho - \alpha_1)\lambda e^x \widehat{A} = 0.$$

Now substituting $\widehat{A}(x) = \overline{P}(x)\, e^x$ in (3.30) and then $\overline{P}'(x) = R(x)$ into the resulting expression we get

$$\alpha_1 \left[\begin{array}{l} (1+\lambda e^x) R''' + (3+4\lambda e^x) R'' \\ +(3+6\lambda e^x) R' + (1+4\lambda e^x) R \end{array} \right] \tag{3.31}$$

$$= \rho \left[R'' + (2-\lambda e^x) R' + (1-2\lambda e^x) R \right].$$

The equation (3.31) is of order three. In order to reduce its order further, we multiply it by e^x and then integrate to obtain

$$\alpha_1 (1+\lambda e^x) R'' + [(2\alpha_1+\rho) + 2\alpha_1 \lambda e^x] R' \tag{3.32}$$

$$+ [\alpha_1 + \rho - (2\alpha_1 - \rho)\lambda e^x] R = 0,$$

where we have taken the constant of integration equal to zero.

The solution of (3.32) for $\lambda = 0$ is given by

$$R(x) = C_5 e^{-x} + C_6 e^{-[(\alpha_1+\rho)/\alpha_1]x}. \tag{3.33}$$

The backward substitution gives the value of $\eta(x)$

$$\eta(x) = -C_5 x + \frac{\alpha_1^2}{\rho(\alpha_1+\rho)} C_6 e^{-(\rho/\alpha_1)x} + C_7 e^x + C_8, \tag{3.34}$$

where C_r $(r = 5, 6, 7, 8)$ are arbitrary constants. The stream function, the velocity components and the pressure field in this case are respectively given as

$$\psi(x,y) = \frac{\mu}{\rho - \alpha_1} y + \left[-C_5 x + \frac{\alpha_1^2}{\rho(\alpha_1+\rho)} C_6 e^{-(\rho/\alpha_1)x} + C_7 e^x + C_8 \right], \tag{3.35}$$

$$u = \frac{\mu}{\rho - \alpha_1}, \tag{3.36}$$

$$v = C_5 + \frac{\alpha_1}{(\alpha_1+\rho)} C_6 e^{-(\rho/\alpha_1)x} - C_7 e^x, \tag{3.37}$$

$$p = p_0 - \frac{1}{2}\rho \left[\begin{array}{l} a_2^2 + C_5^2 + 2C_7 \overline{\alpha} e^{(1-\rho/\alpha_1)x} \\ +2\dfrac{(1-\alpha_1)}{(\alpha_1-\rho)} C_7 \overline{\alpha} e^{(1-\rho/\alpha_1)x} \end{array} \right] \tag{3.38}$$

$$+ \alpha_1 \left[\begin{array}{l} C_7^2 e^{2x} + \dfrac{\rho^2 \overline{\alpha}^2}{\alpha_1^2} e^{-2(\rho/\alpha_1)x} - C_7 \dfrac{\rho^2 \overline{\alpha}}{\alpha_1^2} e^{(1-\rho/\alpha_1)x} \\ \qquad + \left(\dfrac{\rho}{\alpha_1} - 1 \right) C_7 \overline{\alpha} e^{(1-\rho/\alpha_1)x} \\ +C_7 \dfrac{\overline{\alpha}\alpha_1}{\alpha_1 - \rho} e^{(1-\rho/\alpha_1)x} - C_7 \dfrac{\overline{\alpha}\rho^3}{\alpha_1^2(\alpha_1-\rho)} e^{(1-\rho/\alpha_1)x} \end{array} \right],$$

where

$$\overline{\alpha} = \frac{\alpha_1}{\alpha_1 + \rho}, \quad a_2 = \frac{\mu}{\rho - \alpha_1},$$

and the streamline for $\psi = \Omega_3$ is given by the functional form

$$y = -\frac{1}{\varepsilon_2}\left[-\Omega_3 - C_5 x + \frac{\Lambda^2}{1+\Lambda} C_6 e^{-(1/\Lambda)x} + C_7 e^x + C_8\right], \tag{3.39}$$

where

$$\varepsilon_2 = \frac{\nu}{1-\Lambda}.$$

Streamlines are sketched in Fig. 3 for $\phi = \lambda = 0$, $\sigma = 1$, $\mu/\rho = 0.5$, $\alpha_1/\rho = 0.1$, $C_5 = C_6 = C_7 = C_8 = 1$, $\psi = 15, 20, 25, 30, 40$.

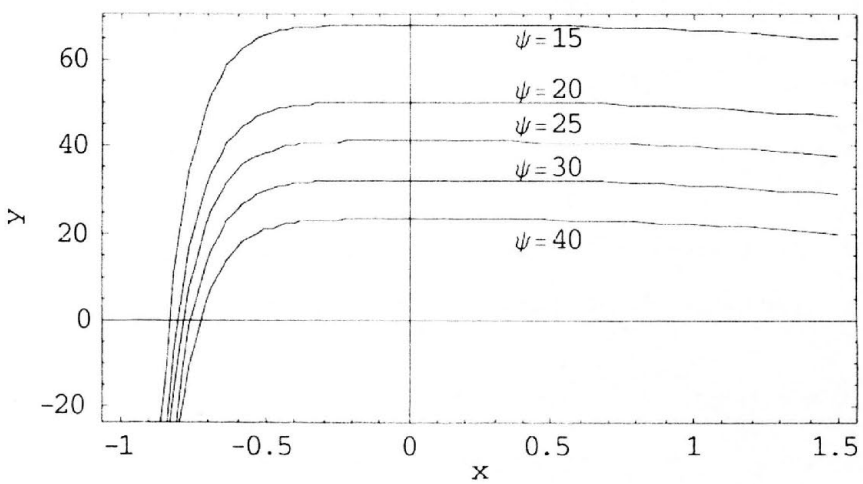

FIG. 3. Streamline flow pattern for

$$\psi(x,y) = \frac{\mu}{\rho - \alpha_1} y + \left[-C_5 x + \frac{\alpha_1^2}{\rho(\alpha_1 + \rho)} C_6 e^{-(\rho/\alpha_1)x} + C_7 e^x + C_8\right].$$

4. Concluding remarks

In this paper, the analytical solutions of nonlinear equations governing the flow for a second-grade fluid are obtained by assuming different forms of the stream function (already used by various authors in different situations). The expressions for velocity profile, streamline and pressure distribution are constructed in each case. Our result indicate that velocity, stream function and pressure are strongly dependent upon the material parameter α_1 of the second-grade fluid. It is shown through graphs that increase in second-grade parameter

($\alpha_1 = 0.15$) leads to decrease in velocity and decrease in second-grade parameter ($\alpha_1 = -0.5$) leads to increase in velocity (see Figs. 4 and 5). Also, the present analysis is more general and several results of various authors (as already mentioned in the text) can be recovered in the limiting cases.

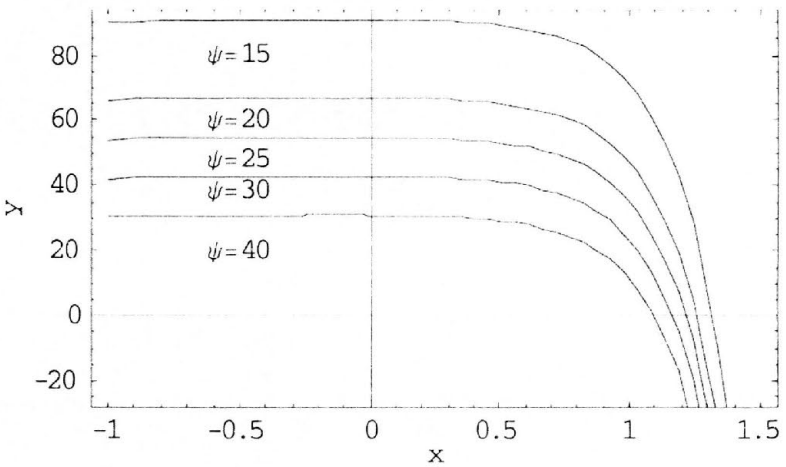

FIG. 4. Streamline flow pattern for negative second-grade parameter for

$$\psi(x,y) = \frac{\mu}{\rho - \alpha_1} y + \left[-C_5 x + \frac{\alpha_1^2}{\rho(\alpha_1 + \rho)} C_6 e^{-(\rho/\alpha_1)x} + C_7 e^x + C_8 \right].$$

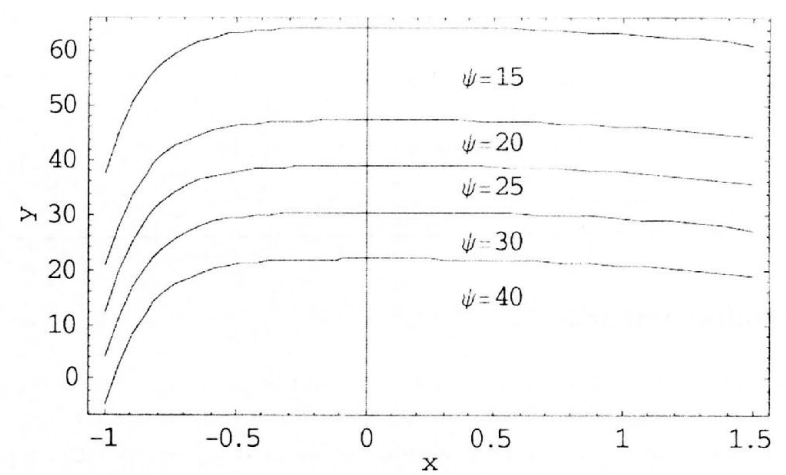

FIG. 5. Streamline flow pattern for positive second-grade parameter for

$$\psi(x,y) = \frac{\mu}{\rho - \alpha_1} y + \left[-C_5 x + \frac{\alpha_1^2}{\rho(\alpha_1 + \rho)} C_6 e^{-(\rho/\alpha_1)x} + C_7 e^x + C_8 \right].$$

References

1. K. R. RAJAGOPAL, *On the boundary conditions for fluids of the differential type*, [in:] A. SEQUEIRA [Ed.], Navier–Stokes equations and related nonlinear problems, Plenum Press, New York, 273, 1995.
2. P. N. NEMENYI, *Recent developments in inverse and semi-inverse methods in the mechanics of continua*, Advances in Applied Mechanics, 2, New York 1951.
3. P. N. KALONI and K. HUSCHILT, *Semi inverse solutions of a non-Newtonian fluid*, Int. J. Nonlinear Mech., **19**, 373, 1984.
4. A. M. SIDDIQUI and P. N. KALONI, *Certain inverse solutions of a non-Newtonian fluid*, Int. J. Nonlinear Mech., **21**, 459, 1986.
5. A. M. SIDDIQUI, *Some more inverse solutions of a non-Newtonian fluid*, Mech. Res. Commun., **17**, 157, 1990.
6. A. M. BENHARBIT and A. M. SIDDIQUI, *Certain solutions of the equations of the planar motion of a second-grade fluid for steady and unsteady cases*, Acta Mech., **94**, 85, 1992.
7. F. LABROPULU, *Exact solutions of non-Newtonian fluid flows with prescribed vorticity*, Acta Mech., **141**, 11, 2000.
8. R. S. RIVLIN and J. L. ERICKSEN, *Stress deformation relations for isotropic materials*, J. Rat. Mech. Anal., **4**, 323, 1955.
9. J. E. DUNN and R. L. FOSDICK, *Thermodynamics, stability and boundedness of fluids of complexity 2 and fluids of second grade*, Arch. Rat. Mech. Anal., **56**, 191, 1974.
10. R. L. FOSDICK and K. R. RAJAGOPAL, *Anomalous features in the model of second order fluids*, Arch. Ration. Mech. Anal., **70**, 145, 1979.
11. A. CRAIK, *The stability of unbounded two-and three dimensional flows subject to body forces, Some exact solutions*, J. Fluid Mech., **198**, 275, 1989.
12. R. BERKER, *Integration des equations du mouvemont d'un fluide visqueux incompressible*, Handbuk der Physik VII, Springer, Berlin 1963.
13. A. CRAIK and W. CRIMINALE, *Evolution of wavelike disturbances in shear flows: a class of exact solutions of the Navier–Stokes equations.*, Proc. R. Soc. Lond., A **406**, 13–36, 1986.
14. R. LAGNADO, N. PHAN-THIEN and L. LEAL, *The stability of two-dimentional linear flows*, Phys. Fluids, **27**, 1094, 1984.
15. S. N. ARISTOV and I. M. GITMAN, *Viscous flow between two moving parallel disks: exact solutions and stability analysis*, J. Fluid Mech., **464**, 209, 2002.

Received January 20, 2003; revised version April 18, 2003.

Institute of Fundamental Technological Research
publishes the following periodicals:

Archives of Mechanics — bimonthly (in English)
Archives of Acoustics — quarterly (in English)
Archives of Civil Engineering — quarterly (in English)
Engineering Transactions — quarterly (in English)
Computer Assisted Mechanics and Engineering Sciences — quarterly (in English)
Journal of Technical Physics — quarterly (in English)

Subscription orders for all journals edited by IFTR may be sent directly to:
Editorial Office
Institute of Fundamental Technological Research
Świętokrzyska 21, p. 508
00-049 Warszawa, POLAND